Title: Clinical application of novel imaging techniques in gastrointestinal surgery

Abstract:

This body of work investigates the current standards of imaging in colorectal cancer surgery as well as the subsequent needs of the field based on the limitations of the technology. It then goes on to identify novel and disruptive techniques that can address these requirements and assess their clinical aptitude. We have covered areas within operative planning and assessment, surgical safety, response to treatment, education, training and mentoring. Textural analysis of CT scan data has demonstrated the ability to identify synchronous metastases significantly earlier than current standards with the potential to alter some patient's course of treatment. The main focus of the work is the introduction of virtual and augmented reality to the medical field. The use of a patient specific three dimensional-model or virtual patient can assist in the planning of surgery through superior interpretation of the anatomy. When combined with the unique surgical rehearsal platform, the operation can be practiced, taught and further investigated with a strong sense of realism. Finally, the headset viewing device provides holographic imagery that aids real-time intraoperative decision making by both surgeons in the operating theatre and remote observers that can be anywhere in the world. There is a strong foundation for this technology within non-medical fields and we have demonstrated a clear level of aptitude and feasibility to allow its adoption.

Impact statement:

The main focus of this work is to address the needs of colorectal surgery and identify uses for new technology that has yet to be adopted by the medical field. As such there are multiple areas where an impact might be made.

The use of textural analysis has been trialled in multiple medical disciplines. Its ability to identify metastases significantly earlier than conventional imaging and add additional information as a radiological biomarker has the potential to alter the methodology of treatment prior to surgery and how patients are followed up after surgery. The ability to know which patients will develop metastases from initial staging CT scans will vastly alter the way in which cancer is treated. Patients that otherwise would not receive pre-surgical chemotherapy may now benefit from additional treatment and patients may decide not to proceed with a major surgical resection if they are aware that it will no longer be a curative procedure. We envisage a textural analysis assessment becoming a necessary part of the multidisciplinary team approach when planning cancer treatment.

The use of a virtual patient is an exciting emerging field within medicine. This body of work has demonstrated the feasibility of creating highly realistic patient specific three-dimensional models that can be viewed by multiple parties simultaneously. These can be used for teaching, they can aid pre-surgical decision making, they can even be used intraoperatively whilst maintaining a sterile field. Using these model's surgeons have the ability to identify subsurface anatomy prior to any incision to improve safety, accuracy and speed of operating. A further development is the potential of the model to more closely measure the tumour response to preoperative chemotherapy that may have a benefit to identify whether the treatment should be continued or stopped earlier than by current means. Using the wearable mobile headsets students can log on to a virtual classroom anywhere in the world and experts can deliver training to even rural or remote areas. Furthermore, using this technology, a surgeon can operate with the device whilst a mentor can not only view the surgeon's field of view but communicate directly with them in real-time.

Finally, the unique training platform that has been developed allows trainees to practice laparoscopic operations within the virtual environment. The technology enables the patient specific models to be loaded onto the platform. This means surgeons can practice or trial certain operations or operative techniques prior to the actual patient operation and students will have access to a bank of different patients comprising a range of pathology and difficulty that will significantly enhance current standards of training.

Table of contents:

Title page

Declaration page

Abstract

Impact statement

Table of contents

Figures and tables

Chapter 1: A narrative review of the current standards of imaging

1.1 Introduction

1.2 A review of current standards of imaging and their applications in colorectal surgery

1.2,1 MRI

1.2,2 Computerised Tomography

1.2,3 Positron emission tomography

1.3 A narrative review of more advanced analytical techniques and the use of biomarkers

1.3,1 Metabolic biomarkers

1.3,2 Molecular biomarkers

1.3,3 Imaging biomarkers

1.4 An introduction to Virtual and Augmented reality

Chapter 2: Aims

2.1 Prediction of recurrence
2.2 Safety in surgery
2.3 Monitoring response to treatment
2.4 Training in surgery

Chapter 3: Objectives

Chapter 4: Textural analysis as a predictive biomarker of colorectal cancer recurrence and metastases.

4.1 Introduction of Radiomics in colorectal surgery
4.2 Aims of the textural analysis study
4.3 Material and methods
4.4 Textural Analysis
4.5 Statistical analysis
4.6 Results
4.7 Discussion
4.8 Limitations
4.9 Conclusions

Chapter 5: Development of a patient specific three-dimensional model

Chapter 6: Validation of the model with peri and intraoperative use

6.1 Uses of virtual and augmented reality in surgery
6.2 Initial use of the virtual surgical patient model
6.3 Review of clinical use

Chapter 7: Development of the haptic training platform

Chapter 8: Conclusions

8.1 Ability of project to achieve aims of MD
8.2 Development of future projects
8.2,1 Model assisted decision making during preoperative planning
8.2,2 Improving intraoperative outcomes
8.2,3 Prospective textural analysis for advanced identification of colorectal liver metastases
8.2,4 Three dimensional measurements of early response to chemotherapy
8.2,5 Evaluation of the advanced surgical rehearsal platform

Chapter 9 Summary

Figures and Tables

Figure 1 Philip Bozzini 1773-1809 and his Lichtleiter

Figure 2 The first radiograph observing a human,1895, Wilhelm Roentgen's wife Anna Bertha Ludwig's hand

Figure 3 A standard CT colonographic image and a three-dimensional reconstruction Ridereau-Zins et al 2012 [12]

Figure 4 A CT image of an enlarged lymph node with high uptake confirmed with FDG-PET CT Kitajima et al 2015 [22]

Figure 5 Image of varying texture distributions, courtesy of Michael A. Wirth, Ph.D. University of Guelph Computing and Information Science Image Processing Group © 2004

Figure 6 Difference in kurtosis (Science Direct.com 2022)

Figure 7 CT texture analysis using the filtration-histogram method: what do the measurements mean? Miles et al [128]

Figure 8 Rectal Cancer patient with liver metastases Devoto et al [98]

Figure 9 Rectal cancer patient with no liver metastases Devoto et al [98]

Figure 10 Kaplan-Meier survival curves for patients with apparently normal appearing liver on conventional contrast-enhanced CT separated by MPP. Survival curves were significantly different for MPP (p=0.018) Devoto et al [98]

Figure 11 The Microsoft HololensTM (Turbosquid, 2021)

Figure 12 Microsoft HololensTM allowing both in person and remote viewing of the same virtual object, (Microsoft Mesh 2022)

Figure 13 Intraoperative use of the viewing device with the wearers view and line of sight displayed

Table 1 The TNM classification of rectal cancer Glimelius et al 2013 [11]

Table 2 Risk factors for colorectal cancer recurrence Zare-Bandamiri, et al. [96]

Table 3 Tumour regression grade by Mandard, Nardone et al [105]

References

Appendix 1: CT Texture analysis of patients who did and did not develop hepatic metastasis

Appendix 2: Mixed Reality SUrgical Resection Guidance MR SURG; Evaluation questionnaire; Statements are evaluated on a 5-point Likert scale: 1 = fully disagree, 2 = disagree, 3 = neutral, 4 = agree, 5 = fully agree

Appendix 3: Video of the patient specific model being viewed prior to surgery

Appendix 4: Video of the creation and intraoperative use of the patient specific model

Appendix 5: Video of a partially co-registered patient model during surgery

Chapter 1: A narrative review of the current standards of imaging

1.1 Introduction

The use of imaging techniques has been at the forefront of medicine for over 200 years from the point when Phillipe Bozzini first used a "Lichtleiter" to observe the human body in 1803, well before Wilhelm Conrad Roentgen used X-rays to further our understanding and ability to both diagnose and treat patients in 1895.

One could argue that imaging has been the single most important technology which has revolutionised patient care in surgery. The impact of the common imaging techniques of CT and USS has been tremendous with the rates of negative-finding operative procedures declining significantly over the last 30 years[2]. Furthermore, imaging forms the central pillar of most treatment decision-making in solid organ cancer surgery.

Whilst the modalities have remained largely the same over recent history (USS, CT, MRI, PET), updates and refinement to the imaging protocols and accuracy of the scanners themselves, eg diffusion weighted imaging have led to further improvements in clinical outcomes.

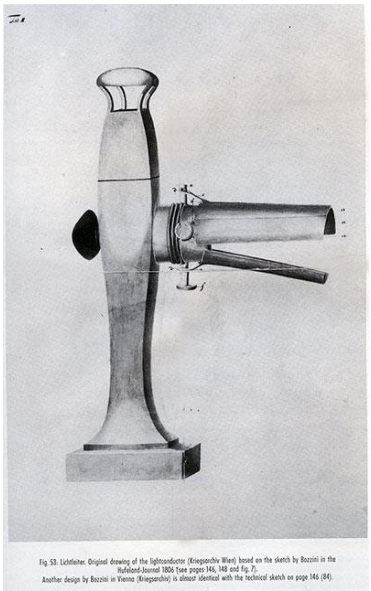

Figure 1: Philip Bozzini 1773-1809 and his Lichtleiter

This body of work attempts to examine several novel imaging techniques to determine their clinical application. Then to evaluate their potential to meet the current needs specific to colorectal surgery. There are several points that disruptive technology may influence the patient pathway from screening and diagnosis to decision making about treatment to treatment itself and then follow up. This can be either as an adjunct to the current system or to supersede these techniques. By working with surgeons, oncologists, radiologists, medical technology experts and engineers we have reviewed current standards to identify areas that can be improved with available technology that has yet to be implemented in healthcare.

Figure 2: The first radiograph observing a human,1895, Wilhelm Roentgen's wife Anna Bertha Ludwig's hand

1.2 A review of current standards of imaging and their applications in colorectal surgery

1.2,1 MRI

The current UK standard for determining the size, spread and dissemination to surrounding lymph nodes of a tumour is the process of staging. Referred to as tumour, nodes and metastases (TNM) staging, for colorectal cancer this involves a multidisciplinary team meeting reviewing computerised tomography (CT) images as well as histological samples to determine the most advantageous treatment options with the addition of magnetic resonance imaging (MRI) for rectal cancer. Surgeons, oncologists and radiologists are present to maintain quorate.[3] Detailed preoperative imaging allows for not only the staging of the disease but using high resolution MRI enables the selection of patients that require preoperative therapy for an attempt at inducing tumour regression. MRI scans gain information on prognostic factors as well as the TNM stage but also depth of invasion into the extramural tissues, the presence of extramural venous invasion and serosal involvement.[4] This allows for a more highly selective approach to patients' treatment. This information can be used to instigate neoadjuvant treatment in those patients with poor prognostic features.[5] Patients that have involved resection margins, that is tumour extension within 1mm of the surgically excised histological specimen, [6] are more likely to have tumour recurrence as well as increasing the likelihood of the disease becoming incurable and causing a poor quality of life with reduced disease-free survival.[7] MRI can also assess post treatment patients following chemoradiation for locally advanced rectal cancer as a percentage will have a complete response and can avoid surgery and opt for ongoing surveillance.[8] However there are limitations in differentiating fibrosis from residual tumour[9]. Commonly this will then require endoscopic histological assessment for confirmation. Different from prognosis, although using some of the same markers, MRIs can aid in assessing predictive factors for post operative disease-free survival. In addition to the TNM stage, the depth of invasion, extramural vascular invasion there is also the presence of inflammatory reaction, mucinous tumour types, presence of pelvic sidewall lymph nodes and the tumour regression grade response to preoperative chemoradiotherapy. These can then determine the need for postoperative adjuvant chemotherapy.[10]

Category	Descriptor
T category	
Tx	Primary tumor cannot be assessed
T0	No evidence of a primary tumor
Tis	Carcinoma in situ: intraepithelial or invasion of the lamina propria
T1	Submucosa
T2	Muscularis propria
T3	Subserosa and perirectal tissue
a*	<1 mm
b*	1–5 mm
c*	5–15 mm
d*	>15 mm
T4	
a	Tumor penetrates to the surface of the visceral peritoneum
b	Tumor invades or is adherent to other organs or structures
N category	
Nx	Regional lymph nodes cannot be assessed
N0	No regional lymph node metastasis
N1	
a	1 lymph node
b	2–3 lymph nodes
c	Tumor deposit(s) in the subserosa, mesentery, or nonperitonealized perirectal tissues
N2	
a	4–6 lymph nodes
b	7 or more regional lymph nodes
M category	
M0	No distant metastasis
M1	Distant metastasis
a	Metastasis confined to one organ or site (eg, liver, lung, nonregional lymph nodes)
b	Metastasis in more than one organ and/or site or in the peritoneum

Table 1 The TNM classification of rectal cancer Glimelius et al 2013 [11]

1.2,2 Computerised Tomography

In addition to the staging of colorectal cancer mentioned previously due to its availability and relative lesser expense CT is used as a screening tool for colorectal cancer detection using CT colonography. This is where dye is placed into the rectum and the patient is manipulated to allow it to coat the bowel before acquisition of the images to allow for a more accurate depiction of the mucosa. Evaluation of the colon is enhanced by its distension with CO2, which distends and unfolds the intestinal wall, thus facilitating the examination for abnormalities of the mucosa, the wall as a whole, and the diameter of the bowel lumen.[12] The main use is in those for whom a colonoscopy is contraindicated.[13] As shown in Figure 3 the images achieved by standard protocols are easily recognisable and require minimal additional training for administration or interpretation. However, with further advances in reconstruction a virtual colon can be created that has the potential to allow further three-dimensional analysis.[12]

Figure 3: A standard CT colonographic image and a three-dimensional reconstruction Ridereau-Zins et al 2012 [12]

Another use is in the postoperative detection of metastases as part of the national guidelines for colorectal cancer follow up. [14, 15] Some

studies have demonstrated a survival benefit in post-treatment patients that have been followed up with CT.[16] However, the results of prior studies suggest that when using the Tumour/Node/Metastases (TNM) classification CT is suboptimal for assessment of local T stage and moderate for N stage disease. Recent advances in CT technology are expected to lead to some improvement in staging accuracy. At present, the main role of CT in pre-treatment imaging assessment lies in its use for the detection of distant metastases.[16] Future aspects of CT use is its fusion with positron emission tomography (PET), as well as dynamic perfusion CT for functional imaging which will be discussed separately.

1.2,3 Positron emission tomography

PET technology combines picomolar sensitivity with high resolution imaging. Positron emitting radiopharmaceuticals are used to target metabolically active and often particularly malignant tissues that will concentrate these substances.[17, 18] Fluorine-18-fluorodeoxyglucose (18F-FDG) PET is a functional molecular imaging technique using the increased glycolysis of cancer cells to visualise both structural information as well as metabolic activity. 18F-FDG-PET combined with computed tomography could help to accurately stage the extent of disease in patients with newly diagnosed tumours.[19] In 18F-FDG PET studies, the maximum standardised uptake value, SUVmax is the most commonly used parameter to measure the metabolic activity of the tumour. In obese patients this must be corrected by lean body mass (SUL), and in paediatric patients, must be converted to body surface area. Metabolic tumour volume is also an important parameter to determine both the local and total tumour burden. Total lesion glycolysis calculated as SUVmean × metabolic tumour volume, provides information about averages. Certain treatment response assessment protocols instead use the SUVpeak or SULpeak of the tumour. Tumour-to-liver ratio and tumour-to-blood-pool ratio can be helpful when comparing studies for treatment response assessment. Dynamic 18F-FDG PET imaging and quantitative analysis can measure the metabolic, phosphorylation, and dephosphorylation rates of lesions but are mainly used for research purposes.[20] PET technology is currently used in the detection of local recurrence of malignancy as well as metastases.

Although highly accurate in both sensitivity and specificity there are limitations. There are financial considerations as well as the availability of the machines as (PET CT) is still of high cost and so PET CT machines are not available in most of centres, in addition there is the potential for false-positive results due to the presence of inflammatory reaction, another limitation as adjuvant chemotherapy may interfere with FDG uptake. PET/CT has limitations in distinguishing the wall layers of the colon and finally a high radiation dose must also be considered.[21]

Figure 4: A CT image of an enlarged lymph node with high uptake confirmed with FDG-PET CT Kitajima et al 2015 [22]

1.3 A narrative review of more advanced analytical techniques and the use of biomarkers

Recently advanced analytical techniques have been developed to extract further information from the data obtained using current imaging techniques or with pharmacokinetic adjuncts. By looking at specific data sets with the ability to extrapolate either a correlation or understanding of the underlying principle more information can be obtained. These are often known as a biomarker. Currently a wide range of biomarkers and potential biomarkers exist across a variety of fields for the management of colorectal cancer. These can be a specific molecule, enzyme or a radiographical finding and can predict outcome or response to treatment. The field is being developed along several fronts with many new innovations happening in the last few years however few have made it into routine clinical practice with others requiring validation.[23] The National Cancer Institute defines a biomarker as a biological molecule found in blood, other body fluids, or tissues that is a sign of a normal or

abnormal process.[24] For the treatment cancer, biomarkers should be objectively measured and evaluated as an indicator of either normal biological processes, or pharmacological responses to a therapeutic intervention.[25, 26] Theoretically the ideal biomarkers being sought can help to determine predisposition for treatment, early detection of disease, and assessment of prognosis.[27] Biomarkers can be grouped into three main categories; metabolic, molecular and imaging.

1.3,1 Metabolic biomarkers

As colorectal cancer results from complex interactions between both inherited susceptibilities, as well as inflammation and environmental/lifestyle-related risk factors, diet and body mass index (BMI), have a major effect. Many studies have demonstrated that an elevated BMI or other metabolic disorders including hyperglycaemia, hyperinsulinemia, dyslipidaemia, type 2 diabetes, and hypertension can increase the risk of colorectal cancer. [28] Adipose tissue acts as a glandular tissue and performs multiple endocrine, paracrine and autocrine functions. It is an important part of the process of neoplastic transformation, specifically in inhibiting the anti-lipolytic effect of insulin.[29-34] The most prominent of the hormonal systems are the adipokines and the insulin/insulin-like growth factor (IGF) axis. These systems regulate, inflammation, angiogenesis, cell proliferation as well as glucose and lipid metabolism.[35] Within these systems; resistin adiponectin, leptin and visfatin have all been associated with either increased clinical risk or mortality and have been validated as biomarkers for colorectal cancer.[23] In addition higher levels of circulating serum IGF1 with an increase of IGF1/IGFBP3 ratio are also associated with an increased risk of colorectal cancer, whilst raised levels of HDL are associated with a decrease. In addition to the increased risk of colorectal cancer hyperinsulinemia and hyperglycaemia have displayed a higher level of mortality with raised levels of IGF2 being associated with an increased overall survival. Finally raised HbA1C levels are an independent predictor of more aggressive proliferation of colorectal cancer.[36]

1.3,2 Molecular biomarkers

An emerging field in the study of biomarkers is the combination of metabolic and molecular biomarkers metabonomics. Metabonomics is defined as 'the quantitative measurement of the dynamic multiparametric response of living systems to pathophysiological stimuli or genetic modification'.[37] Stemming from work with nuclear magnetic resonance spectroscopy these markers can provide information in a systematic time dependent view in response to chemical, environmental or pathological stimuli. [37] By interrogating the effects downstream from the DNA and RNA macromolecules that were previously studied with genomics and proteomics a more specific and tailored approach to prognosis or treatment can be developed.[38, 39] Understanding the three pathways by which colorectal cancer occurs has led to the development of further biomarkers. Epigenetic methylation, chromosomal instability of oncogenes causing mutation and microsatellite instability from ineffective DNA repair have identified epidermal growth factor receptor (EGFR) pathway. This initially led to the first development of patient specific colorectal cancer treatment based on the expression of the KRAS within the pathway.[40, 41] . Mutation of some of the components of KRAS on the EGFR pathway, including KRAS and NRAS codons within a number of exons render the malignant cells resistant to anti-EGFR therapies such as Cetuximab and Panitumumab. This in turn has a direct impact on patient outcomes. [42-44]Further examples of patient specific treatment can be demonstrated based on the expression of the microsatellite instability found within about 15% of colorectal cancers. These can be associated with Lynch syndrome or sporadic mutations of the MLH1, MSH2, MSH6, or PMS2 genes. [45] Microsatellite instability correlates with clinical outcome and so can stratify stage 2 colorectal cancer patients as patients that are node negative with high expression of microsatellite instability have been shown to have better outcome than patients with low expression to the extent that chemotherapy is usually not indicated as it does not affect overall survival. [38, 46] As such it is now indicated in several modern guidelines that testing for these mismatch repair genes should be performed for risk and prognostic stratification. [47] Further emerging biomarkers are MicroRNAs which are short, noncoding RNA segments

that regulate gene expression through interactions post-transcription with mRNA.[48] They can potentially impact a wide range of further effects downstream, both as oncogenes or tumour suppressors. They are involved in multiple pathways that can influence carcinogenesis and tumour disease progression.[49-51] Their role has been described for breast and lung cancer however commonalities exist as their mutations have been found in many generalised targets of cancerous transformation such as EGFR and P53 linking them to expression in colorectal cancer.[52-55]

1.3,3 Imaging biomarkers

Imaging biomarkers are mostly used to detect early disease as well as response to treatment. The simplest version of an imaging biomarker is tumour size. This can be measured by both CT and MRI, however for irregular three-dimensional structures with only 2 linear measurements being taken a true representation of the total tumour volume is not guaranteed. [56, 57] Although reduction in tumour size as a response to neoadjuvant treatment does correlate with a positive response and improved survival. [58] Using dynamic contrast enhanced CT and MRI imaging can demonstrate blood flow which in turn can provide information as a surrogate for angiogenesis. Angiogenesis in colorectal cancer correlates with the development of metastases and decreased survival and so forms a predictive biomarker.[59-62] Another variable observed only on MRI is the degree of fibrosis resulting from chemoradiotherapy. This correlates with the histopathilogical tumour regression grade (TRG), this indicates the level of response to treatment which helps determine the timing of surgery as if minimal or no response is being achieved to a tumour that is borderline with regards to resection margins then it will be preferable to operate rather than attempt further cycles of neoadjuvant treatment.[63] A further independent prognostic indicator that may be used as a biomarker is extramural venous invasion (EMVI) that can be seen on standard MRI images. [58]The presence of EMVI does not affect the staging of the tumour directly but causes the tumour to be considered high risk for recurrence and survival. [64, 65] In addition to current standard imaging with CT and T2 weighted MRI scans specialised sequences and computer algorithms can further delineate

information that may be useful. The diffusion weighted imaging (DWI) sequences may add additional value for evaluation after response to chemoradiotherapy[66, 67] DWI uses the detection of the free random movement of water molecules. Diffusion is the random Brownian motion of the molecules driven by thermal energy. If a medium is perfectly homogenous then the molecules will diffuse in a random and isotropic way, so equal in all directions. But tissues in the human body create a more complex environment, water is divided between intra and extracellular compartments. The relative motion of these molecules can allude to the compartment in which they reside as water molecules that are intracellular are more restricted. The tissues of the human body form a characteristic cellular architecture that have specific patterns of intra and extra cellular components that in turn give characteristic diffusion patterns. The relative proportion of the water distribution between these compartments is affected by the pathologic processes. [68] DWI has been used in the detection of colorectal cancer and its metastases as well as for both response and predictive markers of response after chemoradiotherapy for locally advanced rectal cancer.[69-71]However it has been shown to be less sensitive for hepatic metastases than standard contrast enhanced MRI.[72] DWI can detect changes in the vascularity of tissues and so modifications from anti-angiogenic therapy can be shown before the resulting necrosis alters the size which is one of the standard metrics of response.[69, 73-76] As previously mentioned with PET scans measuring the metabolic response of tissues is possible. Using the understanding of the Warburg effect, where cancer cells preferentially convert glucose into lactate even in the presence of abundant oxygen, has been validated in a variety of cancers.[77-80] This supports the use of [18F]-fluorodeoxyglucose (FDG) enhanced positron emission tomography (FDG-PET) which demonstrates glycolytic flux. [81] PET and CT imaging can also be combined and have been used to predict early recurrence in treated liver metastases. PET and MR imaging have also been combined to increase information on tumour staging, response to chemoradiotherapy and disease recurrence.[82, 83] As the technology has advanced high resolution magnetic resonance spectroscopy (HR-MAS NMR) can combine information about spectra from specific tissues with

chemometric data in real time to indicate active metabolism. It has shown a decrease presence of lipids and glucose with increase of taurine, lactate and glycine in cancerous rectal mucosa to which targeted agents may be developed. [84, 85] The final biomarker reviewed is an application of textural analysis to CT and MRI data. Using existing imaging from CT and MRI scans a further sub-analysis is performed with a computer algorithm to examine the patterns of pixel distribution as a surrogate marker for the tissue's homogeneity. Which in turn demonstrates the cellular structure in terms of organisation and vascularity. Tissues demonstrating increased heterogeneity are associated with poorer survival in certain cancers.[86] Further analysis of this biomarker has been undertaken with regards to feasibility of predicting outcomes in rectal cancer as part of this thesis.

1.4 An introduction to Virtual and Augmented reality

There has been increasing interest in the use of augmented reality (AR) and virtual reality (VR) in healthcare from improving patient awareness and reducing anxiety in the outpatient setting, to early clinical applications.[87] Much of this technology has been developed in other industries, in particular gaming and entertainment, but its application is slowly permeating into surgery with the potential for making surgical procedures more precise and reducing surgical error.[88]
The more commonly used term of virtual reality (VR) describes the use of virtual information and graphics that can only be interacted with within the confines of a 'virtual' world. That is, an entirely computer-generated world only accessible through a computer or device and this in turn limits interaction with the real world whilst immersed within the alternate reality. However, augmented reality (AR), where the user's view of the real world is augmented with additional information, is more applicable during surgery and has potential clinical use. This is where a user can interact with a specific device that allows information from the real world to be viewed by the user as well as adding the additional information. An example is the Microsoft Hololens™, this device has a transparent screen that allows the user to see the real world as normal but then projects holographic images into the user's visual field so that they see and can interact with this information

within the real world. This then naturally leads to the term of mixed reality (MR) is when these two features are combined where by virtual models augment the user's natural view. The concept of mixed reality was defined by Milgram and Kishino in 1994 in which AR is described as a reality-virtual continuum.[89]AR augmented surgery is therefore feasible with intraoperative image guidance whereby the surgeon's view is augmented with imaging derived from the patients anatomy and so is able to identify sub-surface anatomy not visible to the naked eye (the ability to 'see through' an organ akin to "X-ray vision"). Immediate potential clinical benefits include reduction, or even prevention, of blood loss from inadvertent damage to unsuspected vessels such as within liver surgery.[90] In addition there is the ability to define optimal resection margins for both intra-abdominal and percutaneous procedures, as the area of interest may be highlighted defined in three dimensions and continually observed through extraneous tissues.[91, 92] The models can even be accurate enough to provide information regarding tumour invasion into adjacent structures such as vessels.[93] Indeed in certain studies it has been demonstrated that this type of virtual surgical planning can modify the operative strategy in up to 10 % of cases. [92]AR also reduces the 'cognitive load' of the surgeon by providing the required surgical images rather than having the surgeon recall from memory and mentally match the relevant CT/MRI images with their current view.[94] When designing a surgical AR system Sielhorst et al, defined three main criteria that should be met; reliability, the system offers real time accuracy and control in any situation. Usability, minimum interaction between the system and the surgeon. Interoperability**,** generic data and protocols can be used to ensure the system can be used with a variety of equipment and interfaces.[95] Although systems have been evolving for over thirty years there are still substantial hurdles to meeting these criteria. Currently the use of conventional CT or MRI as an intraoperative guidance tool for minimally invasive surgery is impractical mainly due to the impact on the operating room workflow and specifically CT produces exposure to ionising radiation and the strong magnetic field from MRI has implications for staff and theatre design. [92]
We describe the production of a patient-specific VR model that was loaded on to a specialised head-mounted device (HMD) and used during

surgery for colorectal cancer. In addition to the model the surgeon was able to view the original scans and other test results that had been connected to the device whilst also seeing through these images to the surgery being performed. The model was then used for surgical rehearsal with interactions within a simulator that was able to replicate the surgical environment complete with haptic feedback where by the simulator could create different tensions and pressures at the laparoscopic handles used to interface with the device. This meant that subjects were able to identify different structures within the virtual environment by touch as well as visual representation.

Chapter 2: Aims

To understand the aims of this study we have had to identify the current needs in colorectal surgery. These are wide-ranging with multiple factors to be considered, be they accuracy, safety, improved training or health economics. We will set out the current needs that have a potential answer within the most recently emerged technology after discussions with multiple surgeons and the clinical director not only within the base hospital of University College London Hospital, but also speaking with the international community at surgical conferences and via social media.

2.1 Prediction of recurrence

The ability to stratify the risks of a recurrence of cancer will affect the way in which they are treated. Higher risk cancers will invariably be subject to more rigorous treatment or screening.[64, 65] An improved knowledge of these risks will allow tailored treatment specific to each patient to improve outcomes through either improved survival or to minimise unnecessary interventions. Risk factors for recurrence include variables such as age of diagnosis, stage and primary tumour site, T-stage, N-stage, tumour differentiation level, proportion of involved lymph nodes, type of treatment, lympho-vascular and perineural invasion.[96]

Table 2. Univariable and Multivariable Analysis of Prognostic rRecurrence Factors in Patients with Colorectal Cancer

Variables	Univariable HR (95% CI)	P-Value	Multivariable HR (95%CI)	P-Value
Age				
<50 year (reference)	1*		1*	
50-70 year	1.17 (0.84_1.62)	0.211	1.15 (0.84_1.58)	0.331
>70 year	1.811 (1.280_2.561)	<0.001	1.65 (1.09_2.49)	0.012
Sex				
Female (reference)	1		NI	
Male	1.01 (0.78_1.30)	0.946	-	
Site of tumor				
Right and transverse colon (reference)	1		1	
Left colon	0.81 (0.46_1.44)	0.482	0.76 (0.40_1.48)	0.437
Sigmoid	1.18 (0.78_1.79)	0.417	1.17 (0.75_1.81)	0.470
Rectum	1.35 (0.95_1.92)	0.092	1.53 (1.05_2.24)	0.024
Size of tumor				
≤5 cm (reference)	1		1	
>5cm	0.78 (0.58_1.03)	0.098	0.86 (0.62_1.19)	0.360
T-stage				
T1 and T2 (reference)	1		NI	
T3	3.89 (2.43_6.23)	<0.001	-	
T4	9.37 (4.69_18.74)	<0.001	-	
N-stage				
N0 (reference)	1		NI	
N1	1.60 (1.16_2.19)	0.003	-	
N2	2.61 (1.88_3.62)	<0.001	-	
Stage				
I (reference)	1		1	
II	3.61 (2.07_6.31)	<0.001	3.11 (1.65_5.86)	<0.001
III	5.38 (2.88_9.29)	<0.001	4.30 (2.25_8.20)	<0.001
Grade				
Well differentiated	1		1	
Moderately differentiated	1.45 (1.10_1.91)	0.008	1.263 (0.932_1.712) 0.133	0.133
Poorely differentiated	1.71 (1.07_2.73)	0.029	1.39 (0.81_2.37)	0.226
Dissected Lymph node				
>12 (reference)	1		1	
≤12	0.80 (0.58_1.11)	0.195	0.85 (0.60_1.22)	0.391
Proportion of positive Lymph nodes				
≤0.16	1		1	
>0.16	2.02 (1.54_2.64)	<0.001	1.41 (0.85_2.33)	0.170
Lympho-vascular invasion				
No (reference)	1		1	
Yes	2.44 (1.89_3.16)	<0.001	2.03 (1.52_3.72)	<0.001
Perineural invasion				
No (reference)	1		1	
Yes	1.81 (1.40_2.36)	<0.001	1.08 (0.75_1.56)	0.656
Treatment (colon)				
Adjuvant therapy	1		1	
Neoadjuvant therapy	2.04 (1.28_3.24)	0.002	1.4 (0.77_2.35)	0.269
Treatment (rectum)				
Adjuvant therapy	1		1	
Neoadjuvant therapy	1.54 (1.05_2.26)	0.028	1.28(0.80_2.07)	0.291

*, Reference category; NI, Not included

Table 2 Risk factors for colorectal cancer recurrence Zare-Bandamiri, M., et al. [96]

There is also the importance of diagnosing synchronous and metachronous cancers as well as the detection of metastases. Synchronous metastases are defined as distant metastases identified either at the time or within 3 months of initial diagnosis of the primary tumour. Metachronous metastases are defined as the discovery of metastases after a postoperative period of 3 months from the time of treatment.[97] Disease recurrence within 12 months of diagnosis is thought to be due to undetected metastatic disease at baseline.[98]We have identified the use of textural analysis to improve the detection of metastases at diagnosis during the initial tumour staging as well as the potential to predict rates of recurrence from primary rectal tumours.

2.2 Safety in surgery

Both Simulation of adverse outcomes and root cause analysis show that intraoperative errors are often avoidable. [99, 100]Most of these errors are traced back to decision making and so having improved input of information to allow better decisions should improve outcomes. As mentioned, the identification of subsurface anatomy prior to incision should be of great benefit in avoiding excessive bleeding and organ damage, for instance early identification of the ureters during an anterior resection. An added benefit of improved visualisation is the potential to perform more direct surgery to ligate vessels or excise lymph node without excessive dissection in order to first identify the structures before proceeding. This visualisation can not only be performed during the operation but also may have a role in the surgical decision making that happens during the planning of surgery. Understanding the surgical anatomy is critical in both pre-operative planning and intra-operative decision-making. To meaningfully interpret this anatomy with respect to performing surgical procedures, one must be able to translate the visual information obtained from conventional two-dimensional images, currently obtained from CT/MRI, and mentally translate these to the direct operative view.[88] However, this can be challenging, with the potential to misinterpret valuable information. By returning visual data into a more familiar 3D three-dimensional format, anatomical structures and their relevant positions towards each other are more easily understood.[101] Patient specific virtual models may

fulfil these needs allowing for clear interrogation of the anatomy in all six degrees of freedom and we will address the feasibility of model creation and intraoperative use.

2.3 Monitoring response to treatment

With regards to rectal cancers some require down staging with neoadjuvant chemoradiotherapy when it is agreed that the surgical excision margin is threatened by tumour extension.[102]It is important to known if the tumour will respond favourably to such treatment whilst the curative surgery is delayed to decrease the risk of involved resection margins.[7] However if no or minimal response is obtained then surgery will likely be indicated. The problem arises of when to decide that not enough response has been obtained to then change the management as the neoadjuvant treatment is usually given over multiple cycles of several weeks if not longer.[103] Delayed identification of this lack of response not only can allow the tumour to continue to invade into surrounding structures but the unnecessary damage to tissue planes from the treatment will make the surgery more challenging.[103] A problem arises when trying to measure the tumours response to treatment using tumour regression grade as there is a lack of standardisation.[104] The initial scale for rectal cancer was extrapolated from Mandard et al that formed an arbitrary scale based on the formation of fibrosis and residual viable tumour.[63]

Tumor regression grade	Characterization
TRG1	Complete response with absence of residual cancer & fibrosis extending through the tumor margin
TRG2	Presence of residual isolated cells scattered through the fibrosis
TRG3	Increase in the number of residual cancer cells, but fibrosis still predominated
TRG4	Residual cancer outgrowing fibrosis
TRG5	Absence of regressive changes

Table 3 Tumour regression grade by Mandard, Nardone et al [105]

Although the broadly based 5 groups did show correlation with improved survival in both the original oesophageal cancers and rectal cancers also.[106, 107] The response can be measured in several different ways, in addition to the MRI based TRG scale that is clinician dependant and can struggle with differentiation of fibrosis,[104, 108] the RECIST criteria measures tumour size using either CT or MRI to assess volume reduction.[109, 110] This is done by looking at each sectional slice and measuring the longest diameter of the tumour. Thus, for an irregular shaped tumour that has shown volume reduction but just not in those axes that are being measured, important information can be lost as it does not truly represent the tumour volume. One hypothesis we have investigated in this thesis is that in the process of creating patient specific three-dimensional models these included accurate representations of the patient's rectal tumours. Therefore, by measuring true total tumour volume a more accurate depiction of tumour response could be attained.

2.4 Training in surgery

Surgery requires extensive if not life-long training as a skill to perfect. Not only for the surgeon but for theatre staff also. This has multiple obstacles in the allocation of resources and division between service provision and dedicated training. Also, with regards to surgery itself as patient safety must be kept at the highest priority it can be difficult if not inappropriate to allow more junior surgeons to attempt complex resections or manoeuvrers intraoperatively. Although closely mentored trainees do have equivalent outcomes for certain cancer resections this is labour intensive and takes longer per surgery. [111] As training becomes more subspecialised with surgeons concentrating on specific techniques i.e open/laparoscopic/robotic surgery as well as focusing on specific diseases; inflammatory bowel disease, cancer, pelvic floor, invariably the expertise will become more thinly spread amongst the surgical community. Thus, access to surgeons for training will become more difficult. Globally training in rural and remote areas continues to suffer due to the logistical challenges of providing appropriate support.[112]The ability to remotely mentor surgeons using the augmented reality headsets allows for training and the addition of

supportive information in real time over vast distances if required. This can be done using an appropriate headset and voice over internet protocol (VoIP). Both users can share information in an augmented reality setting, in this case the field of view of the operating surgeon. The concept that an expert surgeon can be contactable and able to assist by having instant access to the operating surgeon's current field of view with the ability to be speak and provide telestration by drawing within a shared field of view is a significant advantage for surgical training.[113] One aim of this study was to demonstrate the feasibility of using this technology to improve surgical training in a busy UK teaching hospital. Another use of this technology lies in simulation training with virtual reality. This allows for training across a number of scenarios for surgeons and theatre staff as multiple environments and models can be created.[114] Not only can rare events be simulated with repetition but also difficult technical skills that would have significant consequences if performed poorly in the real world can be practised without risk. For a surgical rehearsal this is done by the creation of a patient specific model. A custom simulator is then used to allow trainees to practice surgical skills interacting with the model. In this way a library of patient models can be built up representing a wide variety of real cases that will span from normal to quite distorted anatomy not normally encountered. A training regime can then be developed where junior trainees can be given easier cases based on the anatomy and build up to more difficult models over time. In addition, as these are models that can be manipulated in the case of cancer resections the tumour can be moved to different sections of the bowel to allow repetition of an operation using the same model but without the trainees gaining an advantage by having prior knowledge for which they would then adapt their technique. This allows for more impartial measurements of trainee progression such as time to completion, efficiency of implement use and excessive force or tissue damage as well as adequate resection margins, all of which can be measured by the simulator. In this study we aim to develop a patient specific virtual reality model that can be manipulated and be placed into a surgical simulator. We then wish to test the initial simulation of a laparoscopic bowel cancer resection with volunteers performing the operation using the above metrics to determine progression and ultimately the validity

of this training method. Finally, we wish to further subdivide the simulation process to determine which aspects will be most helpful to surgeons. The simulator can be divided into three settings. The first is just to simulate a surgical operation whether the model is patient specific, has been manipulated or has been custom created the interactions with the model are the same. The second variant is with the addition of the augmented reality settings. Although strictly speaking this will all take place in a virtual environment making it virtual reality by definition, the simulation is of a real-life surgery where the surgeon is using augmented reality. This additional information that the surgeon would be experiencing were they to operate using the augmented reality device is therefore itself simulated. In this case the patient anatomy is simulated and then the colorised subsurface anatomy of the patient model is displayed superimposed onto the original model. The final variation of the training simulator is the use of haptic feedback. Haptic feedback is the use of touch to translate information, this can be through cutaneous (tactile) or kinesthetic (force) feedback but with laparoscopic surgery only the force feedback can be transmitted to the instruments.[115] The purpose built simulator in this study has the ability to generate haptic feedback to the laparoscopic interface to provide further information about the tissues represented in the model. We aim to test the simulator using all three variants to determine their usefulness as training tools and their reproducibility in an educational environment.

Chapter 3: Objectives

Based on the aims of this project we can summate the objectives we wish to achieve.

- To investigate the ability of textural analysis to predict the development of colorectal liver metastases
- To build a highly realistic, patient specific three-dimensional model
- To test the feasibility of producing a model within a timeframe to enable its input into surgical decision making
- To load a patient specific model and relevant information onto a portable viewing device within that patient’s operation

● To develop a protocol for three-dimensional assessment of tumour response to chemotherapy
● To successfully record surgery whilst using a head-mounted device to demonstrate the ability to live broadcast and use direct remote communication
● To build a novel unique platform with which to interrogate patient specific models as well as train surgical trainees complete with haptic feedback

Chapter 4: Textural analysis as a predictive biomarker of colorectal cancer recurrence and metastases.

4.1 Introduction of Radiomics in colorectal surgery

Building on the principle of using textural analysis as a biomarker we start by looking at the wider field of radiomics. Radiomics in medicine uses novel data characterisation algorithms that aim to extract a large number of quantitative features from medical images beyond the dimensional, uptake, or volume parameters traditionally used in radiology and nuclear medicine. This is used to support decision making and has the potential to uncover disease characteristics that are difficult to identify by human vision alone. Their extraction is based on a rigorous processing chain where each step can greatly influence the result.[116] Texture analysis (TA) is such an example of a novel imaging software that examines pixels on cross-sectional imaging creating novel tumour markers as previously described.[98] TA evaluates heterogeneity or grey-level intensity variations within a 'region of interest (ROI)' that is defined by the user on CT or MR imaging.[117] TA of CT imaging has already shown benefit for diagnosis, staging, determining nodal status and response to therapy in multiple different tumour types.[118-121] With respect to colorectal cancer, studies have shown baseline and post-treatment variations in both CT and MRI texture parameters that correlate with the response to neoadjuvant therapy, primary

disease recurrence and disease-free survival. This in turn is a potential factor for prediction of overall survival.[86, 122, 123] Differences in CT texture have also been shown to detect response to chemotherapy for treatment of colorectal liver metastases,[124] however no work to date at the time of this study has used TA as a biomarker to stratify the pre-treatment scans of rectal cancer patients by susceptibility for development of liver metastases.

4.2 Aims of the textural analysis study

Over the past 25 years, rates of local recurrence for rectal cancer have improved with the introduction of neoadjuvant therapy, and advances in both imaging and surgical techniques, as well as a multidisciplinary team approach.[125] Despite this, a significant number of rectal cancer patients will still go on to develop metastatic disease, primarily to the liver with an inherently worse prognosis.[126] The presence of disease recurrence within 12 months of initial diagnosis of colorectal cancer is thought to be due to undetected metastatic disease at baseline.[98] Current surveillance strategies to detect metastatic disease include serum carcinoembryonic antigen (CEA) and CT imaging at variable intervals from three months to one year, which can often mean a delay to diagnosis. The ability to Immediately identify occult or early hepatic metastasis is of critical importance to guide treatment strategies with the aim of ultimately improving prognosis. As we base cancer staging on the Tumour, nodes and metastases (TNM) model the presence of liver metastases at time of diagnosis and multidisciplinary team meeting can alter the treatment strategy significantly. As a primary resection alone will no longer be curative, the team may choose to begin neoadjuvant chemotherapy and delay surgical resection, or may attempt either a concomitant resection of hepatic metastases and colorectal primary or staggered approach. Knowledge of recurrence of colorectal cancer with the development of liver metastases is also critical as earlier detection will allow for earlier treatment which will improve outcome in patients treated by chemotherapy, and is also associated with better survival in patients treated surgically.[127] Although currently larger liver metastases (greater than about 1–2 cm in size) should be detectable by optimum quality CT or MRI techniques that have a high level of accuracy.

Microscopic metastases (smaller than 1–2 mm in size) are rarely detected and are also rarely discovered during surgery or even after investigation of the pathological specimen.[127] Thus development of a technique to identify the presence of metastases even at a sub-centimetre level before they can be detected by visualisation has the potential for significant implications.

The aim of this project was to produce a pilot study to evaluate a novel radiomic signature using textural analysis for the detection of synchronous liver metastases in colorectal cancer. By examining the serial follow up CT scans of patients during the course of treatment and their surveillance period of 5 years to determine whether TA could identify early changes in those patients who subsequently developed liver metastases. Our hypothesis was that using TA we could detect early changes in liver texture indicating the development of liver metastases before they were then confirmed using conventional high-resolution CT.

4.3 Material and methods

The colorectal cancer registry for a University College London Hospital, a tertiary referral centre, was reviewed. This database is prospectively kept and maintained recording dates of diagnosis, cancer staging, treatment received histopathology and follow up surveillance dates. The patient criteria for eligibility were: histopathologically confirmed rectal adenocarcinoma with initial diagnosis of local disease only on T2 weighted MRI with no evidence of distant metastases on preoperative staging contrast enhanced CT, (TNM Stage III or less). Also, that they then underwent curative resection of the primary tumour without delay or neoadjuvant chemotherapy and that histopathology could demonstrate an R0 resection with a mesorectal plane of excision. The final criteria were that patients required evidence of a full 5 years of follow up surveillance with high resolution CT scans of the chest abdomen and pelvis. The selected patients were then split into two groups those that had developed liver metastases after surgery and a control group of those that did not. The selection process is displayed in Figure 1. In those that developed metastases, the number and size of metastases was not specified in the criteria and any evidence of metastatic liver disease was included. Comparison was made between the two groups to ensure

equivalent baseline characteristics in histopathologically confirmation of rectal adenocarcinoma that underwent identical staging and treatment. The groups were not matched with regards to other criteria as expected the patients who developed metastases would be more likely to have a higher grade showing more advanced primary tumour and have independent risk factors such as a specimen that is positive for extramural vascular invasion (EMVI positive). This information is displayed in Table 1. The primary surgery for both cohorts of patients was performed between 2007 and 2012, to allow for a minimum of 5 years to monitor for disease recurrence. In addition to a review of imaging a hand search review of each patient's medical records at the time of the study was conducted to ensure that there was no current evidence of metastases even if they were beyond the 5-year period of standard follow up surveillance.

4.4 Textural Analysis

Texture is a feature used to partition images into regions of interest, (ROI) and to classify those regions. Texture provides information about the spatial arrangement of colours or intensities in an image. It is characterized by the spatial distribution of intensity levels in a defined ROI and describes the repeating patterns of local variations in image intensity. As such it can not be described for a single point. An example is that an image can be 50% black and 50% white but the distribution of these pixels can vary greatly displaying different texture as in Figure 5.

Figure 5 Image of varying texture distributions, courtesy of Michael A. Wirth, Ph.D.

University of Guelph Computing and Information Science Image Processing Group © 2004

Texture is made up of texture primitives or elements referred to as texels. These are single pixels within a texture that collectively make it up just as a collection of pixels make up an image. Texels however can contain multiple pixels the more pixels it takes to make up a texel and the more subtle differences in the intensities, referred to as tone, between the pixels being measured the coarser the texture becomes. Conversely if each texel is made up of just a few or even a single pixel and the difference between each texel's tone is more distinct then the texture is described as fine. This is a continuous scale and during the analysis texture was set through a filter to image fine, medium and coarse textures within the ROI. Each region within the ROI will have unique texture characteristics and statistical analysis is extensively used to identify repeating patterns. Using a Gray-level cooccurrence matrix. GLCM which is a second-order statistical texture analysis method to the spatial relationship among texels and defines how frequently each combination of texels are present within an image in a given direction and distance. This is defined as the homogeneity of the tissue. By measuring the intensity of each pixel within the ROI we can develop further definitions to describe the texture by placing the results into a histogram for analysis. We can then describe; Mean, the average value of the pixels within the region of interest which changes approximately in proportion to the number of objects highlighted and their mean brightness so darker objects are recorded as more negative. Standard deviation (SD), is measure of how much variation or dispersion exists from the average mean value. A low SD indicates that the data points tend to be very close to the mean and a high SD indicates that the data points are spread out over a large range of values. SD Increases approximately in proportion to the square root of the number of objects highlighted and their mean intensity difference compared to background so both darker and brighter objects are recorded as positive. Skewness, is the next parameter and a measure of the asymmetry of the histogram. The skewness value can be positive or negative. A negative skew indicates that the tail on the left side of the histogram is longer than the right side. A positive skew indicates that the tail on the right side is longer than the left side. A zero value indicates that the values are evenly distributed on both sides of the mean forming a perfect bell curve. The skewness reflects the average brightness of highlighted objects as

predominantly bright objects give positive values, and predominantly dark objects negative values. This will tend to zero with increasing number of objects highlighted and moves away from zero with greater intensity variations in highlighted objects. Kurtosis, is a measure of the peakedness of the histogram. The kurtosis value can be positive or negative. A positive kurtosis indicates a histogram that is more peaked or sharper than a Normal or Gaussian distribution. A negative kurtosis indicates that histogram is flatter. Kurtosis is inversely related to the number of objects highlighted whether bright or dark and is increased by intensity variations in the highlighted objects. As displayed in Figure 6.

Figure 6 Difference in kurtosis (Science Direct.com 2022)

A further description of a texture is its entropy. This is defined as a measure of information content, it measures the randomness of intensity distribution within the ROI. Whilst observing the ROI certain areas will have higher levels of intensity compared to others. When we measure along a line within the ROI, we can find whether the distribution of intensity is equal along the entire line. Such a matrix corresponds to an image in which there are no preferred gray level pairs for the distance vector. Entropy is highest when all entries in P[i,j] are of similar magnitude, and small when the entries in P[i,j] are unequal. Furthermore, the comparison of the histograms created from further segmentation of the ROI gives us a measure of the uniformity of the image. The final parameter that is considered is the mean of positive pixels. This is where the negative values on the histogram created of the ROI are excluded corresponding to the darker areas of the image. All of these parameters will yield unique values related to the ROI selected within an image in this case the liver of the patients and these values are used to determine a correlation between the development of liver metastases.

Texture analysis was performed on the initial staging CT scan of both cohorts using the commercially available TexRAD research software. (TexRAD Ltd, Feedback Plc, Somerset, England, United Kingdom). Contrast enhanced images were used for the analysis and a 10mm section from an area of mid liver that was selected and obtained with a 1s scan duration at a tube current of 300mA at a tube voltage of 120 kVp using a CT Seimens SOMATOM definition AS+ Slice thickness – 5 mm Filter – 31 F Field of view – 40 Portal phase. The same CT scanner was used for the collection of all the staging CT scans in both cohorts. TexRAD uses proprietary software that highlights levels of heterogeneity of the selected tissue within a predefined region of interest and uses histogram analysis to assess and quantify the distribution of grey-levels, coarseness and regularity. It allows for several parameters of heterogeneity to be measured at different spatial scales to be compared and presented as texture ratios enabling quantitative assessment and creates novel imaging biomarkers within a suspected tissue. We used a filtration-histogram technique, where the image is extracted and enhanced along a texture spatial scale filter (SSF) scale corresponding to the size of the ROI. An example of such a histogram is displayed in Figure 7.

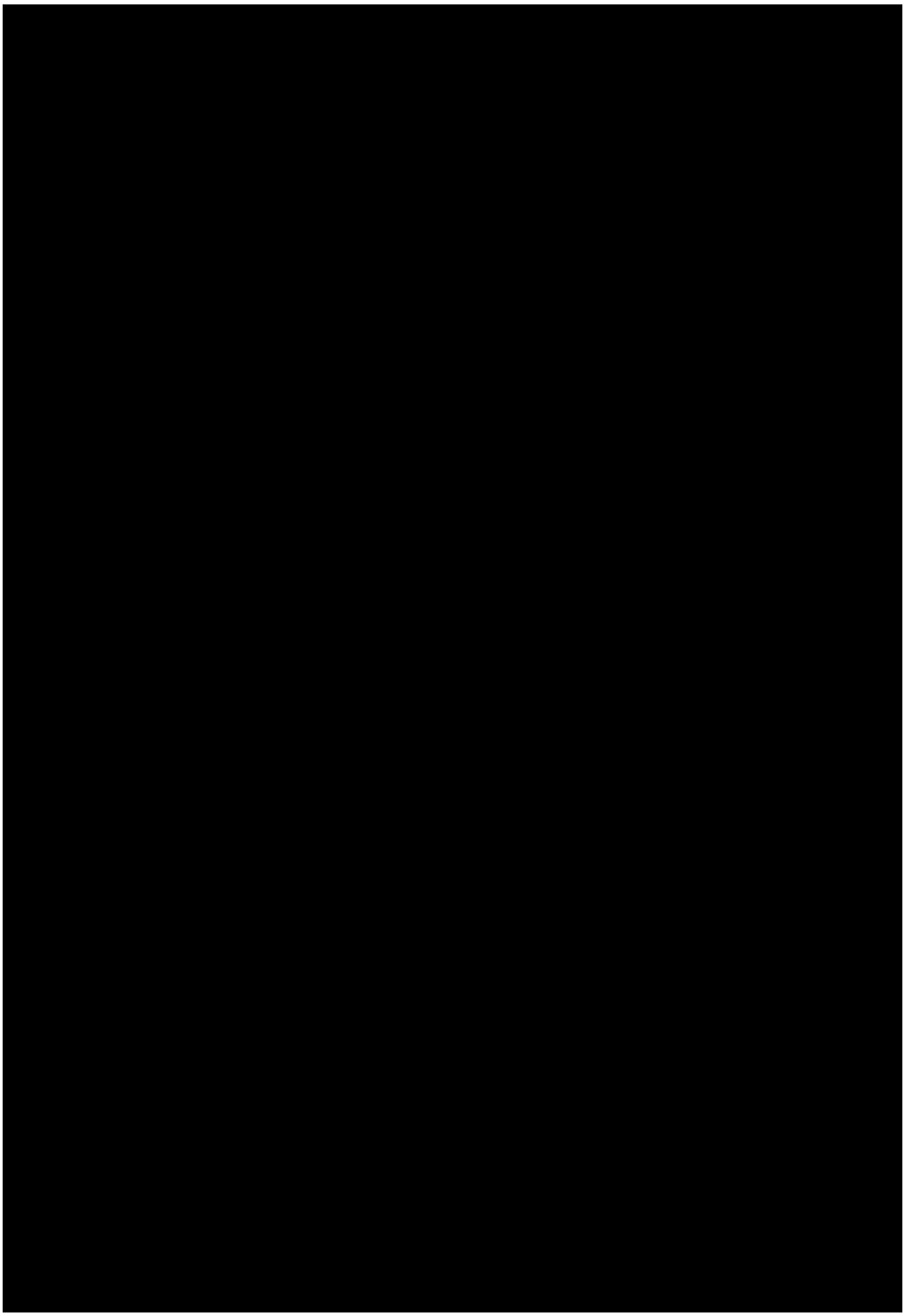

Figure 7 CT texture analysis using the filtration-histogram method: what do the measurements mean? Miles et al [128]

An ROI was initially delineated around the liver outline by hand for the largest cross-sectional area. The TA software automatically identified the entire liver volume within the ROI, and was then refined to exclude the of areas of air with a thresholding procedure that removed any pixels with attenuation values below −50 HU from the analysis. A range of

parameters, including the mean gray-level intensity, uniformity, entropy, mean of positive pixels, kurtosis, skewness, and standard deviation of the pixel distribution histogram were calculated and using Laplacian of Gaussian (LoG) spatial filter. Multiple spatial filter values were set for fine (2.0), medium (3.0, 4.0, 5.0), and coarse (6.0) textures. The TA was performed on the same conventional CT in the control group for comparison. This methodology has previously been described for this technique and its precedent set for clinical application.[129-132] Currently the understanding of the pathophysiology of colorectal cancer spread is that micrometastases from the tumour that have entered into the hepatic circulation block portal flow. This causes localised changes where there is decreased portal venous distention increased hepatic arterial distention and changes of tissue density at a microscopic level with small clumps of cells proliferating throughout the liver. This can then be seen as differences in the homogeneity of the signal and hence the gray-level produced by CT the scanners.[133]

The primary outcome measure reviewed by the study was the ability of TA to identify those patients who would go on to develop colorectal liver metastases. The secondary measure was the time taken to develop those metastases with confirmation using conventional CT scanning from the initial diagnosis using TA.

4.5 Statistical analysis

Statistical analysis was performed by using both IBM SPSS Statistics for Macintosh, Version 23.0 (IBM Corporation, Armonk, NY) and MedCalc version 12.7.2 (MedCalc Software, Ostend, Belgium). Descriptive statistics were used to describe the baseline patient demographic data. For the two diagnostic groups, medians with interquartile range (IQR) were calculated for each texture parameter on apparently normal appearing liver on CT without-filtration and filters of—fine, medium and coarse texture scales. The non-parametric two-tailed Mann Whitney test was used to evaluated the difference between the two groups on the basis of their texture (without and with filtration) besides gender, age and body weight. Box and whisker plots were generated with median, minimum/maximum values and quartiles to demonstrate differences in texture parameters on CT. For the texture parameter diagnostic

threshold to identify the patients who developed liver metastases from those who did not develop liver metastases, this was identified based on area under the receiver-operating characteristics (ROC) analysis along with the values of sensitivity and specificity. The ability of the best CT texture parameter to help predict survival calculated as time to recurrence / Colorectal liver metastases, was assessed using Kaplan-Meier survival analysis. Again, the threshold value calculated for survival analysis was established by using ROC analysis. Survival curves for patients above and below the calculated threshold value were constructed to display the proportion of patients who had not yet developed liver metastases at any given time during the 5 year follow up period. Differences between the survival curves were evaluated using a non-parametric log rank test. For all the statistical analyses, statistical significance was defined at alpha less than 0.05.

4.6 Results

A total of 24 patients were initially included in the study with 12 patients in each group. The different texture parameters calculated both without filtration and filtered contrast-enhanced CT images for the two diagnostic groups are summarized in Appendix 1.
On further review of the medical records of one of the patients in the non-metastatic group, the patient was found to have colonic adenocarcinoma incorrectly recorded in the database as rectal and so was excluded from the study. The prospectively kept patient database was incomplete in certain areas for all patients including in pre and postoperative staging as well as histopathological specimen examination and presence of EMVI.

There were no significant differences found for the texture parameters between the two diagnostic groups for texture analysis without filtration. However filtered texture analysis of the whole, apparently normal appearing liver at baseline CT showed more heterogeneity with significant differences in patients who developed liver metastases compared to a more homogeneous texture quantification in those patients who did not develop liver metastases. At medium to coarse texture filters, the features quantified as mean intensity, entropy,

standard-deviation and mean of positive pixels were the markers of heterogeneity which were found to be significantly higher in patients who developed liver metastases compared to patients who did not develop liver metastases. Particularly the texture differences were more amplified at the coarser filter scale (mean, p=0.044; entropy, p=0.032; SD, p=0.013; MPP, p=0.007) compared to medium filter scales (mean, p=0.044; entropy, p=0.069; SD, p=0.016; MPP, p=0.019).

A demonstration of the active region of interest with the texture analysis applied is shown in Figures 8&9.

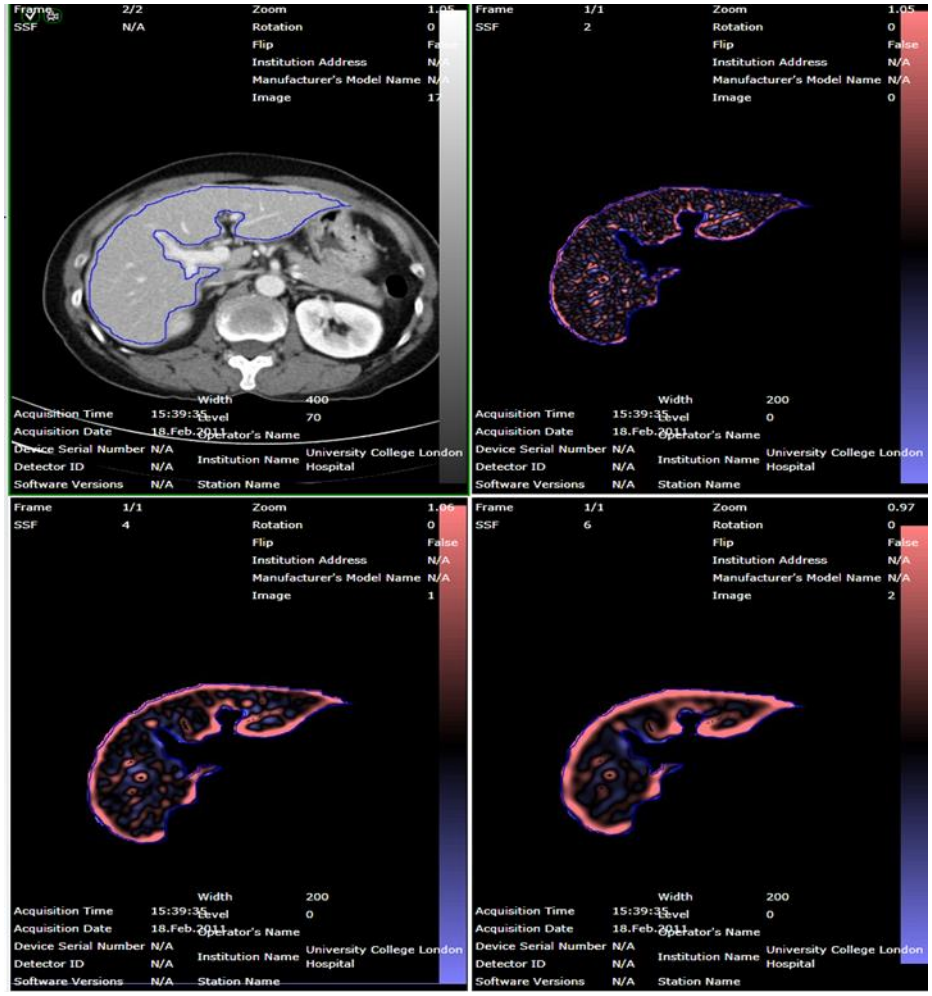

Figure 8 Rectal Cancer patient with liver metastases Devoto et al [98]

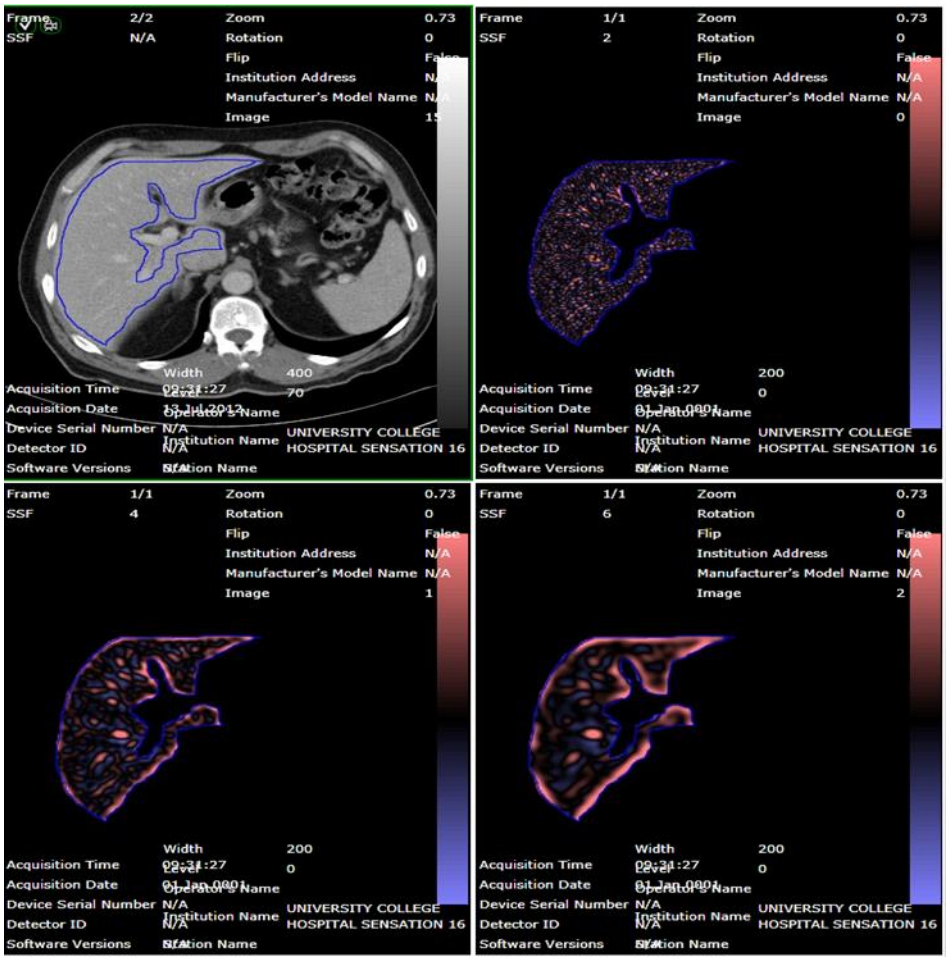

Figure 9 Rectal cancer patient with no liver metastases Devoto et al [98]

At the coarse filter scale, a mean >=9.285 identified patients who developed liver metastases from patients who did not develop liver metastases (area under ROC curve = 0.750, p= 0.044, sensitivity = 83.3%, specificity = 63.6%). Also at the coarse filter scale, any SD >=29.935 identified patients who developed liver metastases from patients who did not develop liver metastases (area under ROC curve = 0.803, p= 0.013, sensitivity = 75.0%, specificity = 63.6%). For the coarse filter scale, entropy >=4.605 identified patients who developed liver metastases from patients who did not develop liver metastases (area under ROC curve = 0.761, p= 0.032, sensitivity = 75.0%, specificity = 63.6%).
And finally for the coarse filter scale, a MPP >=27.8 identified patients who developed liver metastases from patients who did not develop liver metastases (area under ROC curve = 0.826, p= 0.007, sensitivity = 83.3%, specificity = 72.7%). For the survival-analysis, the median time to survival, recurrence / colorectal liver metastases, of the patients was 75.6 months.

12 of the 23 patients followed up developed liver metastases. The shortest time to development of colorectal liver metastases was 7.16 months. Kaplan-Meier survival curves were significantly different (p=0.018) for MPP at the threshold value of >=27.8 this is displayed in Figure 5. Median survival in the poor prognostic group with the MPP >= 27.8 was 15.7 months.

A final important finding is that the average time to development of colorectal liver metastases was 25.04 months (7.16-78.9 SD 21.5) This indicates that from a staging CT scan the textural analysis programme can predict the development of these metastases an average of 25 months and even up to 78.9 months prior to their confirmation with conventional scanning and follow up protocols. Even though they would not be considered synchronous due to the delay, this challenges what we consider to be synchronous metastases. The nature of development of colorectal liver metastases is questioned as there was a significant correlation found with all the patients who went on to develop colorectal liver metastases even ones far later than the average there is the possibility of far-reaching detection for future development.

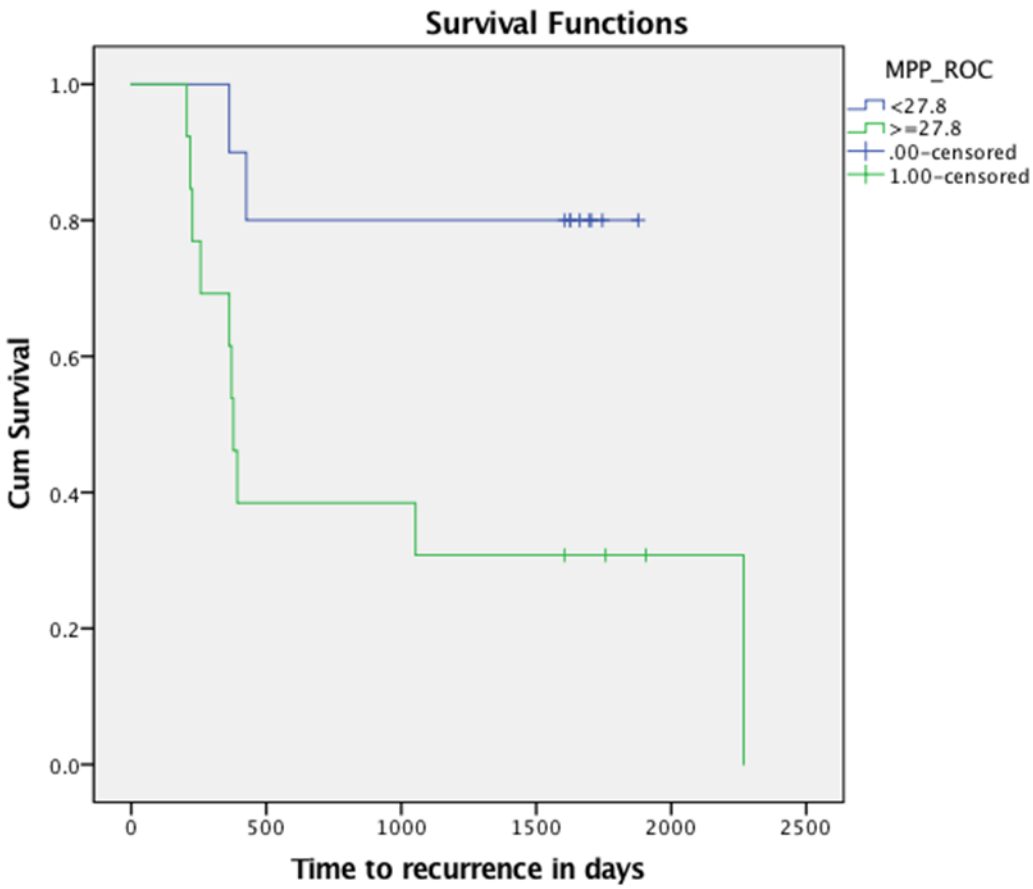

Figure 10 Kaplan-Meier survival curves for patients with apparently normal appearing liver on conventional contrast-enhanced CT separated by MPP. Survival curves were significantly different for MPP (p=0.018) Devoto et al [98]

4.7 Discussion

The results of this initial pilot study demonstrate that TA can potentially predict the development of colorectal liver metastases in patients. Some of these who are due to undergo what is believed to be curative surgery for rectal cancer by identifying subtle changes on the staging CT scan. TA is most sensitive when the coarse filter is applied compared to the medium or fine filters, so when comparing large groups of texels together representing comparison of whole segmented areas of the liver rather than single cells. These changes are not immediately seen on conventional CT scanning used for staging in the United Kingdom, as the changes can not be seen with the naked eye and do not produce a recognisable pattern that can be interpreted by a human observer. The

differences are based on the intensity of the pixels/texels and their distribution as calculated compared to an expected random pattern consistent with homogeneous tissue. When considering the feasibility of using the programme clinically for each new rectal cancer patient, we have demonstrated the ability to perform the analysis in a few hours for each case. Thus, allowing ample time to obtain results between the acquisition of the initial staging scan and the multidisciplinary meeting to decide on the optimal treatment in accordance with best practice in most cases. Also, as this is a largely automated process based on the programme minimal training for interpretation would be involved as there will simply be a threshold limit for the markers that if reached would indicate the presence of metastases. These initial results demonstrate the potential for a specific radiomic signature to detect hepatic metastases in colorectal cancer.

Currently, the risk of metastatic disease developing following an initial curative resection for M0 rectal cancer is determined by the pathological staging of the tumour. Specific tumoural characteristics such as the depth of penetration, the presence of extramural venous invasion and nodal involvement (stage III disease) mandate the use of adjuvant chemotherapy to mitigate the risk of distant disease.[134] However, despite the use of adjuvant therapies a significant proportion of patients with colorectal cancer still develop liver metastases. Surgery is the preferred treatment for liver metastases if they are amenable to resection, but early detection is key.[135] In certain higher risk patients, metastases can often develop within 12 months of the surgical resection of the primary tumour. By definition this is considered synchronous disease, this simply means that those metastases were thought to be present at baseline but are not detected, and reflects the inadequacies of the current imaging modalities used for baseline staging to detect such synchronous metastases.

TA has the potential to provide an alternative and possibly more accurate assessment to detect early distant disease within the emerging field of radiomics. As currently surveillance strategies following rectal cancer resection are variable with no universally adopted consensus on how best to manage patients, TA provides an additional surveillance strategy. This would be not just as a screening tool for patients at their initial

staging where the presence of distant disease would alter their treatment strategy, but also for current specific patients in postoperative follow up considered at risk of developing metastatic disease. By performing TA on the initial surveillance CT scans, it may be possible to detect metastatic disease early enough to surgically resect or ablate the disease. Which in turn would have the potential to significantly affect the patient outcomes. By optimising surveillance and managing distant disease this to could improve survival outcomes through earlier intervention. To consider which patients would be most at risk is a further challenge as currently this is based on historical 'bin models' of staging using tumour depth and nodal disease forming the TNM staging.[136] As more is learnt about the biology of tumours, we believe surveillance strategies would incorporate biological stratification with more advanced analysis techniques such as TA. This pilot study opens the possibility of exciting future work, one potential future study under development is include biopsies to areas which have been identified by TA for pathological validation. This would aid in determining whether early dysplastic or metastatic changes are actually occurring, and the ability of TA to localise specific areas of tissue that are at risk as currently calculations are based on the whole transactional area of the liver. It is one thing to know that a patient is likely to develop liver metastases and would benefit from neoadjuvant/adjuvant chemotherapy, but another to know exactly which area of the liver will develop those metastases and could be amenable to direct forms of treatment.

Ng et al studied the CT features of primary colorectal cancer in relation to 5-year overall survival rate. Tumours that demonstrated less heterogeneity were associated with a poorer survival. We can therefore surmise that the addition of texture analysis to staging contrast-enhanced CT may improve prognostication in patients with primary colorectal cancer not just with respect to distant disease but also by examining features of the primary cancer itself.[86] Similar results were found assessing the pathologic response to chemotherapy in patients with colorectal liver metastases. Lesion uniformity was found to be increased in the good responders while correspondingly entropy decreased. In the poor responders, the opposite effects were observed.[124]

TA was also performed on the MRI scan of the primary tumour and has been previously shown to be a marker of severity in terms of prognosis and treatment response of the pathological specimen.[123, 137] In this case no significant differences were found and not all patients had either had staging MRI scans or had those scans available for analysis so this was not followed up fully in the study. Although there is the potential for assessment of both the primary and liver textures displayed on MRI imaging this would involve a further dedicated study.

4.8 Limitations

Limitations of the study include the small sample size used and the retrospective, non-randomized nature of the selection and assessment of the patients. To better investigate the potential of TA a prospective study will be needed with greater numbers to achieve external validation. Although the software runs a generic, all be it proprietary, computer programme which is universally accepted, prior to the analysis there is some degree of manual segmentation of the scans which is user-dependent. This is due to the analyser selecting the ROI by hand and although in this case the liver outline is fairly well understood and interpreted by most medical professionals there is the potential for a small degree of variability in the outline that is drawn. Furthermore, this study did not compare TA with either PET scanning or MRIs of the liver. As these more advanced imaging modalities have been shown to better detect changes in liver architecture and tumoral activity, they also have the potential to detect liver metastases earlier than current standards and so affect the outcome of treatment decisions, surveillance and overall survival. However currently these modalities are not universally used in either staging nor surveillance and they have an additional relative disadvantage of having huge cost implications. The Texrad software needed for TA does have an initial cost associated with it but then the running of the programme has only the consideration of the few additional man hours required for initiation and interpretation. An interesting future work would be comparison to these modalities or even the addition of TA to MR scans of the liver.

A further point of note is that the small number of patients meant that multivariate logistic regression was not possible considering the number

of variables examined. We also acknowledge that the study was retrospective allowing for the possibility of selection and confounding bias. Finally, the multiple variables, (6 at each of the 6 levels of filtration = 36 variables per patient), assessed by the textural analysis program has the potential for false discovery however we are confident that due to the strong correlation found in the results and the high numerical threshold required by the program to correctly be interpreted as indicating metastases, that these findings are robust. In the study selection we have also identified that the TA was only performed on patients with otherwise healthy livers we do not know how other comorbidities such as cirrhosis might effect the analysis or the interpretation to give erroneous results.

4.9 Conclusions

This initial pilot study supports the hypothesis that in normal appearing liver, texture analysis of the baseline staging CT is more heterogeneous and significantly different in patients who develop liver metastases compared to patients who do not develop liver metastases. Patients that eventually develop metastases have a higher texture-score, while those who do not develop metastases have a more homogeneous liver, with a lower texture-score. TA detects and measures the 'tumour complexity' in CT images and reveals more information than is readily visible to the naked eye. The differences in tissue heterogeneity could potentially be used for more specific risk stratification, prognosis and management for rectal cancer patients. With these promising results of this pilot, further prospective validation is necessary to determine the power of TA in this application. This pilot study has demonstrated a clear indication of the relationship between unique textural features forming a biomarker and the development of metastases and so we are currently planning a follow up study that is prospective with a lager cohort of patients that will be able to fully interrogate the influence of mean intensity, standard-deviation, entropy and mean of positive pixels.

Chapter 5: Development of a patient specific three-dimensional model

A prospectively sourced patient was identified via the University College London Hospital(UCLH) outpatient clinic. They had biopsy proven sigmoid adenocarcinoma and underwent an initial staging CT scan of their chest abdomen and pelvis to be presented at their multidisciplinary team meeting to plan their initial treatment in keeping with current national guidelines.[3] Additional consent was then granted for imagery and video for the purposes of education and research in keeping with UCLH trust policy. These records were then stored in a secure location within Charles Bell House. The initial Digital Imaging and Communications in Medicine (DICOM) data was then downloaded onto an open-source editing platform. The (DICOM) standard is a comprehensive, international standard for medical imaging. DICOM defines a standard medical image file format as well as a metadata model and network services for the storage, transmission, and query and retrieval of objects.[138] The most common DICOM data object is an image file. A DICOM image file consists of both metadata and the pixel data of the image combined into a single file. The pixel data may be encoded using the Joint Photographic Expert Group format or other standard compression methods. The metadata model is standardized by object type, meaning there are different metadata models for a magnetic resonance image, compared to a CT image.[139] However the data is standardised and as such can be exported to multiple open-source platforms to allow further interrogation and editing. For the purpose of the model creation the DICOM data was loaded onto the programme ITK Snap™ (www.itksnap.org). The images were then reconstituted in a standard 2mm axial segmented view congruent with the most common display used within the hospital setting for viewing patient CT scans. Each slice of the CT scan was then reviewed manually and all major organs and vessels within the abdomen and pelvis were defined and separately traced along the x and y axis. In addition to the organs and vessels as the model was to be trialled with respect to decision making in colorectal cancer surgery the cancer was also traced as was the mesorectum. As each slice was the progressed being directly adjacent to the prior image this accounted for the Z axis. This is the process of segmentation. The areas of interest

defined as each organ or vessel being traced were defined using the crop tool to map out the outline of the surface of the organ or vessel being interrogated. Once the entire outline had encompassed the organ or vessel this is defined as a mesh, the internal surface area could also then be calculated for each segment and so once this had been done for every segment a three-dimensional outline could be generated and the internal volume calculated. The resulting model could then be rendered in two ways, either to leave the outline mesh without generating the internal volume sections of the model which would be a surface rendering or to generate a model that includes the information about the volume generating a volumetric rendering. This is more labour intensive and requires more computer processing power than simple surface rendering where the outline of the area of interest is defined but this is then virtually wrapped over a wire frame mesh so that they are essentially hollow. Although the surface renderings are also commonly used to depict three dimensional images, they lack the extra information to allow any kind of virtual interaction such as deformation. As the model being created was due to be loaded onto not only the headset viewing device but also the simulator this would ultimately require interaction that only volumetric rendering could provide. [88] Each individual organ and vessel was then colourised as the original CT images are all in shades of grey depicting their density. The editing programme not only allows for the colourisation of the model but also for a level of transparency for each organ or vessel to be set separately. As part of the segmentation process the biopsy proven rectal cancer of the patient was also rendered separate to the bowel. This was not only then colourised differently to its surrounding bowel but set at a much more opaque level where the bowel was set to be more transparent. In this way when viewing the model in its entirety with all organs in their anatomical positions the cancer could be immediately identified. To add in the surrounding skeletal bony structures 3D Slicer™(www.slicer.org) a separate automated programme was used. Although each bony structure could also have been manually segmented and defined in the same way as described for the other organs and vessels the unique density of the bone allowed for a faster automated process. The same DICOM files were loaded onto the Slicer programme and as these

images depict density using Hounsfield units which are a universally recognised computed tomography attenuation coefficient [140]

Hounsfield unit formula

$$HU = \left(\frac{\mu_{material} - \mu_{water}}{\mu_{water}} \right) \times 1000$$

$$\mu = \text{CT linear attenuation coefficient}$$

As such the denser the tissue to lighter the colour. Bone being the densest tissue is set to the highest Hounsfield score and appears distinctly white. Thus, the programme is able to be instructed to take every pixel within the image of this colour and automatically segment it in every slice to instantly render a three-dimensional image. Once this has been done the image can be interrogated for artifacts where other areas of similar density have been mistakenly captured such as calcifications in vessels. These can then be manually selected and removed to demonstrate a final clean image of the bones. Each organ and vessel are saved as a separate file within the programme and can then be combined with the bony model and viewed together in either programme as a final complete model. As the manually segmented models are traced by hand, they will contain surface errors as the outline will not exactly match the true surface of the organ or vessel. To compensate for this there are automatic smoothing programs that can account for sharp unrealistic angles that would not be found in the true tissue. As such various limits can be selected on the level of angle that is accepted or replaced with a more obtuse angle that gives a smoother averaged view of the organ or vessel. This can be done in either programme however the more the object is smoothed the more information is replaced and the tissue can become less accurate.

Therefor the smoothing process happens over a number of iterations as each time a segment of the outline of the mesh is corrected by the programme that will change the way it joins to the next segment of line and form new angles, some of these will need to be smoothed. A depiction of this would that a square in a basic smoothing programme would be smoothed to an octagon if the correction was set to replace any angle at 90 degrees or less but accepted any angle at 135 degrees or above. Each corner would be replaced with a straight line connecting the two sides thus turning a four-sided shape with four angles into an eight-sided shape. If the programme was then run again accepting on angles over 157.5 degrees this would convert the octagon into a sixteen-sided polygon and so forth until an approximation of a smooth circle was reached. However, if the programme tried to convert a square into a circle it would not know how to correct the angles so severely and be unable to comply and so remove the square entirely. Thus, unconstrained smoothing that is completely automated can remove too much fine detail of anatomy and so must be separated into steps that are reviewed manually for best results,[141] this can be accurate to perform within 0.65mm slices with a 0.3mm overlap. [142] There is a learning curve with the segmentation and a degree of expertise in radiology is required to interpret the CT the initial model required 40 hours of lab work to be created although for surface rendering this would be less. This is an important consideration for the stages of the patient pathway at which the model could be implemented. It is unlikely an individual surgeon or member of a multi-disciplinary team would have such time as to create a model for each individual patient within the constraints of the cancer pathway before that patient was due to be discussed. As the patient had a dedicated research team to produce this model, they were able to have it ready prior to their cancer surgery but not created in time to be discussed at the multi-disciplinary meeting. This process was later outsourced to a private company Visible Patient™ (Strasbourg, France). Simple mesh surface renderings could be completed within 3 working days once the images were anonymised and securely transferred.

With the initial model constructed within the time frame to be used for the patient's surgery it was then loaded onto the Microsoft Hololens™.

This was done in conjunction with the private company Digital Surgery (Digital surgery Ltd, London, UK).

[redacted]

Figure11 The Microsoft Hololens™ (Turbosquid, 2021)

The Microsoft Hololens™ is a stand-alone mixed reality headset viewing device. It is designed to be worn by the operator as a pair of glasses. Images are then projected onto the multiple glass layers giving a seemingly 3D holographic image projected in front of the user. Multiple users can also share image data and so view the same projection at the same time. Sensors within the device detect movement as well as placement with regards to the other users and adjust the projections accordingly allowing the users to circle around an image and if the image has three-dimensional data the image will be adjusted in real time accordingly. For example, an image of a statue correctly loaded onto the device can be circled around all sides could be viewed in all 6 degrees of freedom so including the top and even underneath. However, a picture with only two-dimensional data could be viewed but once an angle too obtuse was reached it could no-longer be displayed similar to viewing a picture hung on a wall. In our case the patient model could be fully interrogated from all angles as well as

manipulated. Other users are acknowledged if within the viewing device's field of vision. Additionally remote users can dial in and still view the shared image. The users are represented with virtual avatars to the other Hololens™ users. Users can communicate via VoIP, (voice over internet protocol), and each avatar's eyeline is visible, allowing the participants to clearly communicate about specific sections of the model.

Figure12 Microsoft Hololens™ allowing both in person and remote viewing of the same virtual object, (Microsoft Mesh 2022)

The Hololens™ application is built using the Unity engine (Unity Technologies, USA), a further open-source computer programme that can write code to edit and manipulate the DICOM image files whether they are the original data from the CT scan or the now edited model, any DICOM dataset can be packaged with the application. On initial launch, a 3D texture is generated from the dataset, and cached to avoid re-generation for subsequent launches. This 3D texture is rendered using volumetric ray marching (volume ray casting), this consists of four steps. First, ray casting, for every individual pixel of the image being displayed, a ray along each line of sight is shot or "cast" through the

volume. The irregularly shaped volume is considered to be enclosed by a bounding primitive made up of a number of simple geometric cubes that are used to intersect the ray of sight and the volume.

Figure 13 Intraoperative use of the viewing device with the wearers view and line of sight displayed

The second step is sampling, along the part of the ray of sight that intersects the volume, equidistant sampling points are selected. Normally the volume is not perfectly aligned with the ray of sight, and sampling points will usually be located in between the voxels. Thus, it is necessary to interpolate the values of each sample from its surrounding voxels (commonly using tri-linear interpolation). The third step is shading, for each sampling point, a transfer function is used to retrieve the standard Red-Green-Blue- Alpha (RGBA) colour and gradient of their illumination is created. The RBGA is how the information about the colour of an object is encoded with blending of these colours to project the desired effect. The alpha refers to the opacity of each pixel allowing for layers of pixels to be built up to provide information about shading.

The gradient of the shading represents the orientation of the surfaces within the volume. So, by adding the shading the viewer appreciates the 3D nature of the object. The samples are then shaded according to their surface orientation and the location of the light source that will be created within the projection. As this is a virtual model a virtual light can be generated from any angle and appear to illuminate the model depending on how the voxels are shaded. Multiple light sources can be generated but this will add to the complexity of the projection and increase the processing power requirements. The final step is the composition, after all the sampling points have been shaded, they are composited along their ray of sight. This results in the final colour and illumination value for the pixel that is currently being processed. This composition is derived directly from a rendering equation that calculates the total amount of light emitted from each point along the ray of sight and is similar to placing multiple acetate sheets on an overhead projector. This work flow direction ensures that masked or obscured parts of the volume do not affect the resulting pixel. The method of central differences was used to approximate the gradient between voxels, the 3D pixels containing information about volume in the 3D texture, and use this to provide normalisation shading for a single directional light [95]. The addition of shading to the model using the simplest simulated light source allows greater appreciation for the anatomy highlighting the depth perception for this display as the Hololens™ projects a 2D image in front of the wearer that the brain interprets as 3D. Hand calibrated 1-dimensional transfer functions were used to highlight and separate each layer. This is a function of interaction with the model within the Hololens™. Pre-set hand motions allow various functions to be completed including loading the model loading CT scans displaying and manipulating the model. All these can be done with gestures within the Hololens™ field of view. In this way the surgeon can remain sterile whilst still interacting with the viewing device.

The model was also able to be loaded directly into the training simulator. This was a purpose-built device constructed by Generic Robotics (Generic Robotics Ltd, Reading, UK), it combines a virtual reality headset with an arcade style control system developed with the surgical team at UCLH. As the simulator was designed to mimic

laparoscopic surgery the control panel has laparoscopic instrument handles that the user can grasp and move in all six degrees of freedom. These are held in place by a system of motorised connectors that can vary the resistance with which the handles can be moved. They are also able to vibrate giving the user a degree of haptic feedback. This will give the user a sense of density and weight of the tissue being handled as the motors adjust the feedback in real time depending on the actions of the virtual instruments being controlled by the user. For example, if the user grasps the laparoscopic handles and uses them to virtually control the laparoscopic grasping device in the simulation and virtually picks up an item, the motors in the panel will push the handle down to simulate the natural weight of the virtual object. If the virtual object is light the motors will exert less force than if the object was heavy. Similarly if the user is advancing the laparoscopic handle to push the virtual instrument further into the simulation and the virtual instrument is pressing against a part of the model that is pliable such as the bowel, the bowel will deform in the simulation mimicking the real tissue and the motors in the handles will provide a degree of resistance such as one would feel in pressing against real tissue, however if the virtual instrument was pressed against a simulated bony structure of the model then the motors would lock entirely as the bone would not deform in reality.

Chapter 6: Validation of the model with peri and intraoperative use

6.1 Uses of virtual and augmented reality in surgery

The first operation performed with augmented reality was by Kelly et al in 1986 for neurosurgery.[143] Surgeries where there is little or no movement or deformation of the tissues involved naturally lend themselves to this technology as the image that is required can be projected directly to the operating microscope without the need for continuous calibration or to orientate the augmented image with the surgeon’s view. This is the process of registration where the model is aligned with the anatomy it represents in all three axes. Further advances have been made in the fields of ENT[144] orthopaedic,[145] and maxillofacial surgery.[146] The first general surgical operation was described by Marescaux et al in 2004, A laparoscopic assisted

adrenalectomy.[147] These types of operation provide difficulty from both the movement of tissues during surgery due to direct operative deformation and the physiological movements such as breathing and the patient's heartbeat. Even the establishment of pneumoperitoneum can shift intraabdominal organs by a significant amount.[148] There are also added difficulties in registration of the image due to movement of the target organs from the time of the preoperative scan which acquired the data to create the augmented view. To the time of the operation itself.

Although systems have been evolving for over thirty years there are still substantial hurdles to meeting these criteria. Currently the use of conventional CT or MRI as an intraoperative guidance tool for minimally invasive surgery is impractical mainly due to the impact on the operating room workflow and specifically CT produces exposure to ionising radiation and the strong magnetic field from MRI has implications for staff and theatre design.[92]

In previous cases, an augmented view was projected onto the patient to help with the decision of port placement.[149] However the projected view differs from the surgeon's perspective and has to be compensated.[150] This was initially overcome with the use of semi-transparent mirrors,[151] but these cannot demonstrate a 3D image and so are unsuitable for laparoscopic surgery. Binocular head mounted displays have been trialled to provide a 3D image that aligns with the surgeon's perspective in the past but these were found to be too heavy and cumbersome.[152] More recently light versions of monocular displays such as Google Glass™ have been used,[153] but again these did not provide a stereoscopic display, causing a degree of parallax error from the viewpoint of the surgeon. It has been demonstrated that a stereoscopic display is superior to monoscopic for use in laparoscopic surgery.[154, 155]

Augmented reality attempts to address some of the limitations of minimally invasive surgery such as the hand eye disconnection due to viewing a screen as well as the reduced depth perception from the 2D view.[94] Although 3D models have been displayed on tablets intraoperatively the use of the headset greatly improves these limitations. The other main drawback of minimally invasive surgery is the lack of haptic or tactile feedback that provides information on

texture, weight and pulsation. Robotic systems are being designed to include haptics for feedback from tissue and the 3D model has the ability for tissue characteristics to be mathematically calculated to respond to distortion. This has been shown to predict organ movement with respiration,[92] we have been able to demonstrate good correlation with this using the simulator. Beyond the use within theatre, both the information and the surgeons view can be broadcast in real time or recorded. This concept has been used to mentor local surgeons by international experts around the world, who were able to conduct real-time consultations during live surgery.[156] This may have useful applications where surgical expertise is limited by geographical or financial constraints. In addition to this there is the use within surgical training to accelerate learning curves of increasingly complex procedures. For example, intra-operative augmented reality can be used to provide an immersive experience for surgical trainees alongside reference videos, imaging and text. Surgical trainees can also operate using the Microsoft Hololens™ whilst their trainers can remotely observe their trainees' progress. Telestration, the process of drawing directly on to the live video, can be performed using the Hololens™ image to further aid in teaching.[112] This can be limited by the need for high-speed internet connections and the current technology allows for only basic hand drawn lines painted onto the image with a finger or stylus.

6.2 Initial use of the virtual surgical patient model

Application for intraoperative use was granted through the surgical auditing lead (Mr KD). The initial virtual reality model was viewed on a desktop monitor. This was the surface rendering as no interactions with the model involved deformation simply viewing and rotation. This showed the important components of the anatomy including the axial skeleton, colon and mesentery with tumour highlighted in the right colon, important adjacent anatomical organs. This allowed for surgical strategy planning and understanding which potential organs were at risk during the resection. The information was clearly displayed compared to that of the 2D format where there is the potential to lose or misinterpret information even when viewed by senior

radiologists.[93] The augmented reality model was seen initially by the surgical team prior to surgery. (Video appendix 3) The display included the standard CT images as well as the augmented reality model. The user was able to move between the views by turning their head in different directions. During the surgery, the user was able to turn on the head-mounted display and view the overlaying anatomy. This was a laparoscopic procedure so the actual operating was performed on a separate screen belonging to the laparoscopic stack, but the overlay imaging helped for initial port placement and triangulation. (Video appendix 4)

Due to the limitations of the graphics processing unit (GPU) performance on the Hololens™, many optimisations and rendering quality reductions were undertaken, including empty space skipping, reducing the viewport size, down-sampling, and reducing the ray marching resolution.[157, 158] Parameters for these optimisations can be adjusted at runtime via voice commands, allowing to user to have full control over performance vs imaging quality. This is an ongoing refinement as in certain circumstances very high image quality is required to define structures when operating near them for example dissecting near the inferior epigastric vessels or ureters. Here the refresh rate of the model image does not have to be as fast as there is very little head movement that comes with greater concentration focusing on only one important area. However, when operating far away from the areas of interest it is more important for the model to be processed at a faster refresh rate as if the model is skipping and jumping it can become distracting. One potential solution to this issue to provide better imaging quality can be achieved by rendering the model offline and streaming it as a live video to the Hololens™, this requires far less processing power as the image has already been produced and merely needs to be displayed. Another solution is to improve the GPU output by recruiting further processing units from "cloud computing", this is where servers that are off site are accessed via the internet and can combine their processing power with the Hololens™.
Video footage has been recorded simultaneously of the model in use by the Hololens™. Footage displays the use of the initial patient model and

its segmentation. The use of the augmented reality display has been shown to provide CT data as well as the model and also footage shows further surgery using the volumetric rendered model in use during surgery being interrogated as well as a surface rendering being directly overlaid onto the patient anatomy (Video appendix 5). We have found that due to the weight of the headset it was not suitable for continual wear during a prolonged operation with an anecdotally reported maximum time for comfortable wear of 20 minutes. However, we have found as the image is cashed, the headset can be taken off and replaced multiple times without needing to reload the model causing minimal disruption to the surgeon. In this way the model can be loaded for the important stages where it will be most useful. Through this initial use we have been able to demonstrate the feasibility of using the Microsoft Hololens™. We have produced a manually-aligned, stereoscopic 3D image of patient-specific anatomy produced from routine patient imaging data, that can be viewed during live surgery. Whilst the user/surgeon must wear a headset on to which the sensory input is loaded, this is only required at specific stages of the surgery rather than throughout the procedure. The model can be interrogated and manipulated by the surgeon using hand movements or voice commands in six degrees of freedom, whilst remaining sterile in the operating field. Organs can be moved or removed and made transparent for easier understanding and visualisation. Having an immediately accessible and accurate model of the patient could be a useful tool during complex surgery. This is the first time a patient-specific model has been created for use during a live colorectal cancer operation, as well as the addition of original CT images onto the user's interface. This model demonstrated relative accurate alignment and acted as an anatomical reference when required by the surgeon particularly for port placement. In addition to the model the surgeon was able to view the original scans and other test results that had been connected to the device whilst also seeing through these images to the surgery being performed.

6.3 Review of clinical use

This initial feasibility study is promising but with the current technology there are a number of limitations. Firstly, the production of the model to yield the highest level of detail is time-consuming and whilst machine learning algorithms are able to automate the process somewhat, there is still reliance on manual segmentation if the models are to be used in precision surgery. As mentioned, private companies are available to reduce the workload of the surgical team but the financial implications may limit the uptake of the technology unless a significant improvement in outcomes can be demonstrated to justify additional costs. Next the alignment or co-registration of the model is not yet ideal. We relied on anatomical landmarks but this does not account for subtle patient movements, respiration, changes in the pressure of the pneumoperitoneum and table movements. This challenge has been addressed in part by the use of fiducial markers. These are radio-opaque markers that can be placed on the patient at the time of image acquisition.[159] They are placed in specific reproducible landmarks of the patient's surface anatomy, often bony prominences as reference points. By using multiple markers simultaneously, the position of the patient can be aligned with the equivalent virtually placed markers corresponding to their real-world counterparts. This allows real time registration of instruments when the patient was intraoperatively scanned with repeat MRIs that would update the model with each scan.[91] This method however requires use of intraoperative MRI which would limit its use for most operating theatres. Acquiring an up to date intraoperative image for the model has also been possible using both CT and ultrasound scans.[92] More advances have been made recently with optical tracking of skin markers allowing registration of a volumetric rendering during laparoscopic surgery that did not require MRI imaging.[160] Further work has been using fiducials intraoperatively to compensate for the rigidity of the model. Using automated augmented reality registration and finite element modelling (FEM) coupled with optical imaging of fluorescent surface fiducials. FEM allows simulation of soft tissue behaviour, taking into account the mechanically modelled properties of parenchyma, internal tubular structures, and tumours. This biomechanical model is expected to predict inner deformations by propagation of the observed surface changes.[160] Additionally, fiducials placed inside an organ or target

tissue intraoperatively build a 3D picture within the model and their position can be tracked with a near infrared spectrum camera. The combination of the FEM computer algorithm and the known 3D positions of the fiducials are used to update the model in real time showing deformation of the tissue.[161]
Finally, the headset devices will need to be improved for more prolonged use in theatre. Currently, they are adequate for short periods but become uncomfortable due to their weight after some time. The next generation of such headsets appear encouraging in this respect.

Chapter 7: Development of the haptic training platform

After the initial creation of a 3D patient specific model and its use intraoperatively using augmented reality, we expanded the model's capabilities by developing a dedicated training platform. As the model was created using generic open-source programmes it had the ability to be utilised by other software and hardware as it was compatible. However, one of the important discoveries using the model for training and interrogation was the lack of haptic feedback. There was no sensation of touch giving information on tissue density, texture and malleability. Furthermore, there was no readily available platform to use to test the model in this way. Although a few programmes do exist that can include haptic feedback none had a surgical style of interface that would resemble an operation. As such we have worked with Generic Robotics (Generic Robotics Ltd, Reading, UK) to develop a unique operating system to allow fully immersive surgical rehearsal with patient specific models. Initially the Unreal Engine 4 programme, (Epic Games Inc, North Carolina, USA) was used to add the haptic information to the patient model. The files containing the fully rendered volumetric meshes were loaded onto the Unreal Engine 4 programme where additional information could then be implanted into the model. In the Unreal Engine environment data can be added to create and manipulate gravity and so information of the model's response to this virtual stimulus is required. Each organ has its own mesh and being largely homogeneous will have similar parameters throughout that can be added. The generic values of tissue densities for fat, muscle and bone etc are commonly

known and so when applied in the correct combination to simulate each tissue will be a close approximation for each organ. The attachments of each organ assuming no additional adhesions are also known so each organ can be fixed in the model relative to each other. Thus, we have organs that are placed in a certain part of the body fixed to known structures that when manipulated will deform accordingly and will deform based on the forces applied including gravity and their composition, i.e. bone will not deform very much at all but a more pliable organ such as bowel can move significantly. Although at this time each organ has an average density based on its cellular make up, for example a liver will be mostly made of hepatocytes which will have an average value for density, but the areas of bile ducts and hepatic veins are ignored. With further programming and segmentation of each organ it will be possible to then split these into finer and finer detail that delineates anatomy including blood vessels, lymphatics calcifications and scar tissue etc. Once this additional information was added to the model it was then ready to be loaded onto the surgical platform.

Using a virtual reality headset, (Oculus Quest 2, Meta Platforms Inc, California, USA) a virtual environment resembling a hospital theatre operating room can be created and the arcade style surgical training platform that has two laparoscopic handles is then used to perform the operation within this virtual environment. The laparoscopic handles connect to a series of motors that monitor the forces created by the user in all six degrees of freedom. In addition, the handles are also surrounded by resistors that can constrict the shafts of the handles to provide varying degrees of friction. This will relay the impression of the resistance encountered in the virtual environment. When the virtual instrument is moving through air in the virtual operation there will be no resistance and so the real-world laparoscopic handle will be allowed to move freely. When the virtual instrument encounters a virtual organ, the resistors will then start to constrict the laparoscopic handle initially with minimal friction as the organ will have a degree of deformation before becoming more compacted and resistant. As this happens the friction will increase on the handle. When encountering bone in the virtual environment, in practice no perceivable deformation will take place, thus the motors of the laparoscopic handles will lock not allowing any further travel in the direction going into the bone but the handle will be free to move back

away from the bone. Finally, to mimic the weight of the various tissues again the resistors are engaged when the virtual instrument is shown to be holding or lifting an object in the virtual environment. When this happens there is increased friction on the laparoscopic handles when moving the virtual object against gravity but the motors run freely when moving the object with gravity, the motors will even attempt to move the object according to the virtual objects place in the environment to rest at a point where gravity is cancelled, i.e. an object will fall until it comes to rest. In this way a highly realistic virtual environment has been created that mimics a laparoscopic operation.

Next a protocol was developed to test the platform. A cancer has been modelled in a separate mesh as part of the creation of the initial patient model and has had its own characteristics added using the Unreal Engine 4. It is denser and so feels firmer and deforms less to mimic the real tissue. Thus, when manipulating the bowel virtually using the platform when encountering the cancer, the user should be able to recognise this as the haptic feedback will differ. The surgical training platform has the ability to measure a number of metrics that can delineate operative proficiency. These metrics include; total time taken to complete a task, efficiency of use of instrumentation and distance of simulated resection margins. As a trainee becomes more proficient performing the operation we would expect total time taken to simulate identifying the cancer and resect the appropriate length of bowel to decrease. Also, we would expect proficiency of the instrument handling to increase, so fewer unintentional movements with a more direct path drawn from the instruments starting points to there destination to complete each stage of the task. Finally with clear identification of the tumour we would expect appropriate resection margins at least one centimetre from the tumour. Although in reality appropriate resection is determined by multiple factors including blood supply, and tension on the tissue this model has yet to simulate active blood flow. The major blood vessels to the organs have been simulated and a record can be taken if they are cut or put under extreme tension during the simulation but we are yet to recreate the conditions necessary to determine end organ oxygenation. The protocol was then developed where by a trainee would begin the simulation with two laparoscopic instruments to select of which there were multiple varieties available. Graspers were selected and the trainee

would be asked to identify where in the bowel the tumour was situated. They were then asked to select appropriate resection margins either side of the segment of bowel containing the tumour. Whilst developing the protocol we were aware of the phenomenon of learning by repetition. In this case once the trainee has performed the task of locating the tumour in the bowel initially through haptic feedback and visual clues of the differences in deformity created when manipulating the tissue, they would then be able to remember the location of the tumour. On repeated simulations the trainee would be able to improve their speed and accuracy simply by remembering where the tumour was in the bowel and where resection margins should be drawn based on their previous outcome. This would then mimic the effect of improvement through simulated practice. This was overcome by using the ability to move the tumour to a new segment of bowel with each successive simulation so that it would have to be found anew each time using the conventional methods already described. The final stage of the protocol was then to add the transparency and colourisation abilities of the model. The initial simulation mimicked the normal appearance of the body tissues and organs that would be encountered during an operation. During this finial stage the bowel could be made either semi or fully transparent and the tumour brightly coloured to aid in identification. We anticipate that when performing either the simulation or a real bowel resection for a bowel tumour, identification of the tumour and thus the appropriate planes of resection would be significantly faster and more efficient if the surgeon was able to see a brightly coloured marker delineating the tumour. The simulator has the ability to do this instantly, whereas the technology exists in the real world when using the augmented reality headset to produce the mixed reality model and overlay it in front of the surgeon's view. Providing minimal displacement of the patient's internal organs has taken place since their CT scan from which the model would have been derived then the virtual marker should indicate with some degree of accuracy where to find the expected tumour. However as previously mentioned we know that patient organs do move both spontaneously and as a result of the initiation of surgery thus the registration of the model with the native anatomy can become out of sync and misrepresent the true current location of the tumour during surgery.

Initial feedback from the training protocol has been positive. Both advanced colorectal surgeons and surgically naive volunteers have been able to utilise the platform. The haptic feedback of the instruments has been described as realistic and the surgical environment created in which to perform the virtual surgery is intuitive such that even the surgically naïve can perform the task with minimal introduction as displayed in Appendix 2. We have gained ethical approval for a prospective non randomised trial where by volunteers are split into surgically naïve and surgically experienced trainees and asked to follow the surgical training protocol to identify the bowel tumour and mark appropriate resection margins either side. The task will then be repeated with the tumour moved to a different location. The task will be performed 3 times with and 3 times without the aid of haptic feedback through the instruments. Finally, the task will be performed with the visual aid of the colorised model. Metrics of efficiency will be recorded to demonstrate the learning curve and any proficiency gained through repeated simulated training.

Chapter 8: Conclusions

8.1 Ability of project to achieve aims of MD

Looking in turn at each of the initial aims that have been stated we can assess the ability of the project to address these issues. Firstly, with regards to better predicting colorectal cancer recurrence and the detection of synchronous metastases, we have made a significant finding with regards to the usefulness of textural analysis. This technology is not currently widely used and we have been the first institution to attempt to validate its use in this manner based on a systematic review of the literature being performed finding only 11 papers at the time of experimentation. Although we acknowledge this is only a pilot study with small numbers of patients, the extremely high concordance found with 100% of subjects scoring above the threshold for metastases is promising for the success of the planned future experimentation. We feel that this technology applied using the protocol developed for this project by examining the initial staging CT scans of rectal cancer patients at their

MDT meeting will detect synchronous metastases which would have shown up as a recurrence a number of months earlier. This will invariably alter the course of treatment for most of the T1, T2 and T3 staged rectal primaries as they would likely receive adjuvant or neoadjuvant chemotherapy rather than a single surgery with curative intent. As a result, we would predict improved disease-free survival and overall survival.[162] Although, as stated with the current state of the technology the location of the metastases can not be predicted thus making a pre-emptive liver resection impossible. However, the benefits of early detection of metastases and the administration of neo-adjuvant chemotherapy prior to any attempt at hepatic resection for resectable hepatic metastases has been demonstrated.[127, 163] We would also hypothesis the extrapolated benefit of early intervention. Although no benefit to survival has been demonstrated with systemic reviews of the literature for early versus delayed intervention for incurable hepatic metastases.[164] However these studies have only looked at known metastases located with conventional techniques and compared the effects of chemotherapy between when the metastases are first detected and when they become symptomatic. This has been an average of 5 months and 179 days respectively in the two main trials that have previously investigated this issue and been reviewed by meta-analysis.[165] With an average of 18 months in this study prior to discovery let alone symptomatic progression we feel that there is a strong possibility that a significant benefit will result from early treatment.

Next with regards to safety in surgery, although no quantitative data has been generated subjective feedback has been positive. Demonstration of subsurface organs including blood vessels has been indicated to result in decreased blood loss from inadvertent damage during port placement.[92] The videos of the patient models in use have demonstrated the ability to replicate these findings and clear indication of tumour boarders will invariably aid surgery and surgical decision making. Simulation of surgery prior to the actual operation has demonstrated an overall increase in proficiency.[166] And with the score of proficiency used being the Global rating score, (GRS), that includes markers such as respect for tissues and tissue damage, we can surmise that surgery will also be safer. (Table 4)[167]

	SCORE 1	SCORE 2	SCORE 3	SCORE 4	SCORE 5	Exposure of biliary region and adhesiolysis	Dissection of the cystic pedicle and critical view	Dissection of the gallbladder	Overall
RESPECT for „tissue"	Frequent unnecessary force on tissue or caused damage by inappropriate use of instruments	→	Careful handling of tissue but occasionally caused inadvertent damage	→	Consistently handled tissue appropriately with minimal damage to tissue				
TIME & Motion	Many unncessary moves	→	Efficient time / motion but some unnecessary moves	→	Clear economy of movement . Maximum efficiency				
Instrument **HANDLING**	Tentative moves / inappropriate use	→	Competent use of instruments / occasionaly inappropriate	→	Fluid moves with instruments				
Depth **PERCEPTION**	Constantly overshoots, swings wide, slow correction	→	Some overshooting but quick to correct	→	Accurately directs instruments in correct plane				
BIMANUAL dexterity	Uses only one hand, poor coordination between hands	→	Uses both hands but does not optimize their interaction	→	Expertly uses both hands to provide optimal exposure				
OVERALL impression	Novice	→	Experienced	→	Expert				

Table 4 Example of an operative specific Global Rating Score Moldovanu et al [167]

With regards to preoperative surgical planning again we have demonstrated the feasibility for the use of the virtual model. The headset viewing device is portable and requires minimal setting up for activation. The model can be viewed through the device by multiple parties without any specific training and we know that 3D visualisation is better interpreted than the current traditional 2D views.[93]The turnaround time between acquisition of the patient staging CT scan which would be the basis for any future models and creation of a usable model for surgical planning which would be a surface mesh rendering is only a few, average 3, days. Thus, we feel that in the majority of cases this would not delay the initial MDT meeting. We acknowledge that the cost of producing a model when outsourced to a private company of a few hundred Euros has to be taken into account, however given the initial incidence spending in the U.K. in the first year of colorectal cancer treatment is between £14,196-19,187,[168] we feel that this cost can be justified for a significant number of cases due to its potential benefits. We would also expect costs to be driven down as the technology becomes more widely available and better business cases can be negotiated if the utilisation of the model was widely accepted by the

hospital allowing for economy of scale through mass purchasing. Finally, there has been development in the field of artificial intelligence with respect to model creation. We have already described the use of an automatic programme for density-based segmentation of the model with respect to bony structures. However, full model creation for maxillary surgery has also been achieved with an average model creation time of 1.7 minutes and have then gone on to be assessed by expert users to have comparable results. [169]

When considering the monitoring of response of colorectal cancer to initial neoadjuvant treatment we feel the three-dimensional aspect of the virtual model will be inherently more accurate at measuring changes in volume than the current standard of measuring the single largest diameter in a cross-sectional image unless that image is perfectly spherical. We theorise that more subtle changes can be identified sooner to allow for a more confident decision in cases where surgery is being delayed for neoadjuvant treatment. In cases where patients do not respond to chemotherapy, surgery is there for performed earlier without waiting for completion of the full course of neoadjuvant treatment. By being able to make these decisions sooner there will be less delay for the non-responding patient cohort and ultimately a benefit from performing the surgery earlier.[170] Although not directly studied in this project we have generated a protocol for a future project to confirm the superiority of the 3D model before assessing the ability to prospectively assess response to treatment.

When assessing the aims to address surgical training, the use of the model and headset do have a number of applications. At the undergraduate level similar models have been used to demonstrate anatomy.[171] The anatomy can then be manipulated and interrogated for a greater understanding. The relative cost and ease of procurement compared to a comparable lesson using a cadaver is much less as once the model is created it can be stored and reused. According to Reuters commoditise a cadaver can cost between $3000-5000 and will then need to be stored with all necessary ethical and legal requirements of both handling and disposing of human tissue. Although cadavers in general can last about 6 years with some museum specimens being preserved for much longer, in order to fully teach all the relevant anatomy, manipulation mostly in the form of dissection is needed. Thus, a new

cadaver is normally required for each group of students each year. Comparing the cost of the headsets at £3,349 including VAT per unit and the cost of each model which can be created for free using open-source programmes or a few hundred Euros if outsourced the use of a virtual model has distinct advantages. In addition, a library of anatomical subjects can then be built up over time to demonstrate both normal and specific variants of anatomy with near instant access. These models can also be shared over great distances to remote learners. We have shared access to the model between sites of the UCL university campus, Charles Bell House, Foley Street, London, W1W 7TS, UCLH hospital, Euston Road, London, NW1 2BU, Digital Surgery main office, City Road, London, EC1V 2QY, the Royal National Stanmore hospital, Bolsover Street, London, W1W 5AQ and the IRCAD centre, Place de L'Hopital, 6700, Strasbourg. Further use of the model in surgical training is with the development of the surgical training platform. The uses vary widely from introduction of students to a virtually simulated surgical operating theatre, to highly specific surgical rehearsal for complex operations for higher surgical trainees. This method of training also has several advantages over traditional methods in that metrics of proficiency can be recorded for more accurate and personal feedback about trainee progression. Also, sessions can be recorded and played back for more intense scrutiny and assessment. Finally, the same operation can be repeated at leisure for convenience and with a model library being collected we anticipate that models with the appropriate level of difficulty on which to perform a simulated operation can be selected to match the level required for the trainee. For example, a straight forward right sided cancer resection would be selected for a first-year surgical registrar but a complex resection for a recurrent rectal cancer with previous chemoradiotherapy and associated diverticular disease would be for a final year trainee or junior consultant. The initial feedback has been positive in the use of the platform and standard metrics for speed, instrument efficiency, instrumental control, excessive force and tumour resection margins have all been captured successfully. We expect to be able to demonstrate the increased proficiency gained by successive training using the platform.

8.2 Development of future projects

8.2,1 Model assisted decision making during preoperative planning

One of the next stages to utilise the model is to assess its effectiveness to aid the decision making during the planning stage of a patient's care, specifically the MDT. We have demonstrated the use and feasibility of using the model with the headset viewing device in an MDT setting. We know that three dimensional images are easier to understand than two dimensional ones recreating the three-dimensional image and so we hypothesise that using the 3D model in an MDT setting will aid the decisions concerning treatment. Factors such as the ability to achieve adequate resection margins from a tumour, proximity to other organs and vessels and the presence as well as position of effected lymph nodes will all influence the decision to attempt a curative operation with or without neoadjuvant chemotherapy. These decisions then need to be agreed upon between surgeons, radiologists and oncologists. We would look to test the use of the model with a simple questionnaire given to each team member of the MDT team. The initial decision made by each participant in the usual way after consulting patient notes and traditional CT and MRI scans would be recorded with a level of confidence, and then again after consulting the viewing device with the model. In this manner we would record whether using this additional information source would change the decisions of the participants and ultimately the congruousness of the team. As with certain difficult cases the team members might be split in opinions over how to proceed, we would wish to know if this added information could facilitate the team all coming to the same conclusions.

8.2,2 Improving intraoperative outcomes

As we have demonstrated the use of the model intra-operatively, we now intend to assess and quantify the usefulness of the system. There are several features to assess including; the overlay or registration of the model onto the patient anatomy during the operation. The additional information such as original CT scan data that can be accessed by the viewing device. And the cooperative interface where a second surgeon can both see and communicate with the wearer of the viewing device. We have developed a generic questionnaire that can be applied to each of these three scenarios where by each feature is used singularly during

an operation or all features together. (Appendix 2) Ultimately the aim would be to prove whether or not these features reduce morbidity and mortality from surgical operations with secondary end points being the length of time taken to complete the operation and the total blood loss. This would require a sizeable prospective randomised trial as the complication rate for colorectal surgery is relatively low.

8.2,3 Prospective textural analysis for advanced identification of colorectal liver metastases

Textural analysis has shown significant promise in the ability to detect colorectal liver metastases. The pilot study performed in this project has now led to a prospective trial of colorectal cancer patients. Newly diagnosed patients will have a textural analysis of the staging CT scan of their liver to predict the development of colorectal liver metastases. They will then need to be followed up to see the concordance of the predicted results with their disease-free survival. This will allow the refinement of a threshold value for which any patient above a certain level will be deemed to have synchronous liver metastases. If this is then proven with a suitably high power of study the next stage would then to be consider changing the management of these patients depending on the result of their textural analysis. We would postulate a further study where the patients with predicted liver metastases who would otherwise have a favourable outcome and would be intended for a curative resection would receive an alternate course of treatment primarily neoadjuvant chemotherapy. Although the study could be randomised into two cohorts of those that do and those that do not receive additional treatment it could not be blinded due to the use of chemotherapy agents and the unethical delay of intended curative treatment for a placebo group. Follow up would again be of disease-free survival and mortality based on a Kaplan-Meier curve.

8.2,4 Three dimensional measurements of early response to chemotherapy

One further use of the model is with regards to response to chemotherapy. Currently no consensus exists for measuring the response of rectal cancer. Dworak et al have developed a tumour regression score

based on pathological response to chemoradiotherapy derived from the Mandard scale for oesophageal cancer response.[63, 106] The gold standard is to measure and summate the longest singular diameter for each slice of no more than 5mm of the MRI scan, the RECIST criteria. A further study in which we are currently engaging is the comparison of volumetric model measurements to the standard summation of longest diameter in known rectal cancer patients. In this study known rectal cancer patient have been selected from a prospectively kept database that have already had neoadjuvant chemotherapy. Pre and post treatment MRI scans have then had three-dimensional models created with the exact volumes of the rectal cancers calculated. These patients' MRI scans are then assessed by two independent radiologists who measure the summated single largest diameter to calculate a percentage tissue response. The aim of the study is to determine if there is any significant difference that can be displayed between the two methods. If the current standard can measure a similar percentage reduction to the full volume calculations from the models, then there will be no change in the management of the patients. We hypothesise that although the full three-dimensional calculations will represent a more accurate depiction of the tumours response to tumour it may not prove significantly different from the single largest diameter's extrapolation to be of benefit. The results are ongoing and the study will need to reach sufficient power to be able to conclude the feasibility of the model's use. This determination will be based on the fact that although the full volumetric calculations will be more accurate than the single measurements, however the number of patients required may preclude the model's clinical usefulness. As the number of patients required to be included so that a single case is able to demonstrate a difference between the two methods that would alter the final result and alter that result significantly enough to even effect management may be too high to justify routine model creation for every case based on the cost and time consumption. However, there may be a niche use in selected cases of indeterminate response using the current criteria.

8.2,5 Evaluation of the advanced surgical rehearsal platform

With the development of the advanced surgical rehearsal platform current testing is underway to demonstrate, quantify and refine improvement in surgical skills. We have been granted ethical approval by

the University College London ethics board for human experimentation, (Z6364106/2022/01/71medical) with regards to having volunteers both surgically trained and surgically naive demonstrate progression. A protocol has been developed with use of the platform and the additional aid provided by the overlay of the model and the haptic feedback. Volunteers would attempt a laparoscopic colorectal resection using the platform with repeated attempts to demonstrate identification of the tumour within the bowel and selection of appropriate tumour resection margins. The metrics of time, efficiency of instrument handling, organ damage, instrument control with the surrogate of off-screen instrument time and resection margins from the tumour can all be recorded. The scenario will be repeated several times initially without augmentation, then with the colourised model overlay and finally with haptic feedback enabled. A comparison will be made for each added variable to calculate and quantify the benefits if any of each one individually. We hypothesise that repeated simulation of the task will improve outcomes across all metrics however with the addition of an augmented colourised model the time taken to complete the task should be significantly decreased as the subject will instantly be aware of where the tumour is in the bowel and should also have a better idea of where to place the resection margins. Finally haptic feedback should call the attention of the subject to drifting instruments that might start to cause organ damage and will help confirm the tumour location by the difference in tactile feedback but no further significant increase in speed is expected over the colourised model. These results and continued subjective feedback from the participants will help refine the realism of the platform to aid training at various levels from medical students to advanced surgeons as any number of simulations of varying difficulty can be created.

Chapter 9: Summary

Novel imaging techniques and technological advancements continue to evolve at a near exponential pace with processing power doubling about every 18 months. Often these leaps in technology are not translated to the medical field. Careful and systematic testing is required to guarantee patient safety however a paradigm shift is also required in the acceptance of new technological advancements by the medical profession. We hope to have adequately displayed some of the newest fields within surgical imaging and the possibilities that they might achieve. Our aim has been not only to address the current issues faced but also to inspire the uptake and acceptance of these technologies, with near limitless possibilities we hope that the only limit to our advancement is what we can imagine to create.

References

1. Bercovich, E. and M.C. Javitt, *Medical Imaging: From Roentgen to the Digital Revolution, and Beyond.* Rambam Maimonides Med J, 2018. **9**(4).
2. Sabhnani, G. and S. Tomar, *Negative laparotomy rates in acute abdomen: a declining trend.* International Surgery Journal, 2016. **4**(1): p. 323.
3. NICE guideline. 15 December 2021; Available from: https://www.nice.org.uk/guidance/ng151.
4. Brown, G., et al., *Preoperative assessment of prognostic factors in rectal cancer using high-resolution magnetic resonance imaging.* Br J Surg, 2003. **90**(3): p. 355-64.
5. Smith, N. and G. Brown, *Preoperative staging of rectal cancer.* Acta Oncol, 2008. **47**(1): p. 20-31.
6. Adam, I., et al., *Role of circumferential margin involvement in the local recurrence of rectal cancer.* The Lancet, 1994. **344**(8924): p. 707-711.
7. Jhaveri, K.S. and H. Hosseini-Nik, *MRI of Rectal Cancer: An Overview and Update on Recent Advances.* AJR Am J Roentgenol, 2015. **205**(1): p. W42-55.
8. Smith, J.J., et al., *Assessment of a Watch-and-Wait Strategy for Rectal Cancer in Patients With a Complete Response After Neoadjuvant Therapy.* JAMA Oncol, 2019. **5**(4): p. e185896.
9. Xu, Q., et al., *MRI Evaluation of Complete Response of Locally Advanced Rectal Cancer After Neoadjuvant Therapy: Current Status and Future Trends.* Cancer Manag Res, 2021. **13**: p. 4317-4328.
10. Saklani, A.P., et al., *Magnetic resonance imaging in rectal cancer: a surgeon's perspective.* World J Gastroenterol, 2014. **20**(8): p. 2030-41.
11. Glimelius, B., et al., *Rectal cancer: ESMO Clinical Practice Guidelines for diagnosis, treatment and follow-up.* Ann Oncol, 2013. **24 Suppl 6**: p. vi81-8.
12. Ridereau-Zins, C., et al., *CT colonography: Why? When? How?* Diagn Interv Imaging, 2012. **93**(1): p. 2-9.
13. Spada, C., et al., *Imaging alternatives to colonoscopy: CT colonography and colon capsule. European Society of Gastrointestinal Endoscopy (ESGE) and European Society of Gastrointestinal and Abdominal Radiology (ESGAR) Guideline - Update 2020.* Endoscopy, 2020. **52**(12): p. 1127-1141.
14. Sali, L. and D. Regge, *CT colonography for population screening of colorectal cancer: hints from European trials.* Br J Radiol, 2016. **89**(1068): p. 20160517.
15. Liu, S.L. and W.Y. Cheung, *Role of surveillance imaging and endoscopy in colorectal cancer follow-up: Quality over quantity?* World J Gastroenterol, 2019. **25**(1): p. 59-68.
16. Tan, C.H. and R. Iyer, *Use of computed tomography in the management of colorectal cancer.* World J Radiol, 2010. **2**(5): p. 151-8.
17. Frackowiak, R., *Positron Emission Tomography and Autoradiography: principles and applications for the brain and heart*, in *J Neurol Neurosurg Psychiatry*. 1986. p. 848.
18. Arulampalam, T.H.A., et al., *Positron emission tomography and colorectal cancer.* BJS (British Journal of Surgery), 2001. **88**(2): p. 176-189.
19. Vaarwerk, B., et al., *Fluorine-18-fluorodeoxyglucose (FDG) positron emission tomography (PET) computed tomography (CT) for the detection of bone, lung, and lymph node metastases in rhabdomyosarcoma.* Cochrane Database Syst Rev, 2021. **11**(11): p. Cd012325.
20. Sarikaya, I. and A. Sarikaya, *Assessing PET Parameters in Oncologic (18)F-FDG Studies.* J Nucl Med Technol, 2020. **48**(3): p. 278-282.
21. Hetta, W., G. Niazi, and M.H. Abdelbary, *Accuracy of 18F-FDG PET/CT in monitoring therapeutic response and detection of loco-regional recurrence and metastatic deposits of colorectal cancer in comparison to CT.* Egyptian Journal of Radiology and Nuclear Medicine, 2020. **51**(1).

22. Kitajima, K., et al., *Clinical significance of SUVmax in (18)F-FDG PET/CT scan for detecting nodal metastases in patients with oral squamous cell carcinoma.* Springerplus, 2015. **4**: p. 718.
23. Devoto, L., D.S. Keller, and M. Chand, *A Narrative Review on the Current Application Biomarkers in the Management of Colorectal Cancer.* Journal of Molecular Biomarkers & Diagnosis, 2017. **8**: p. 1-4.
24. Young, P.E., et al., *Early detection of colorectal cancer recurrence in patients undergoing surgery with curative intent: current status and challenges.* J Cancer, 2014. **5**(4): p. 262-71.
25. Strimbu, K. and J.A. Tavel, *What are biomarkers?* Current Opinion in HIV and AIDS, 2010. **5**(6): p. 463-466.
26. *Biomarkers and surrogate endpoints: Preferred definitions and conceptual framework.* Clinical Pharmacology & Therapeutics, 2001. **69**(3): p. 89-95.
27. Tanaka, T., et al., *Biomarkers for Colorectal Cancer.* International Journal of Molecular Sciences, 2010. **11**(9): p. 3209-3225.
28. Aleksandrova, K., K. Nimptsch, and T. Pischon, *Influence of Obesity and Related Metabolic Alterations on Colorectal Cancer Risk.* Curr Nutr Rep, 2013. **2**(1): p. 1-9.
29. Ma, Y., et al., *Obesity and risk of colorectal cancer: a systematic review of prospective studies.* PLoS One, 2013. **8**(1): p. e53916.
30. Prieto-Hontoria, P.L., et al., *Role of obesity-associated dysfunctional adipose tissue in cancer: a molecular nutrition approach.* Biochim Biophys Acta, 2011. **1807**(6): p. 664-78.
31. Hursting, S.D. and S.M. Dunlap, *Obesity, metabolic dysregulation, and cancer: a growing concern and an inflammatory (and microenvironmental) issue.* Ann N Y Acad Sci, 2012. **1271**(1): p. 82-7.
32. Greenberg, A.S. and M.S. Obin, *Obesity and the role of adipose tissue in inflammation and metabolism.* The American Journal of Clinical Nutrition, 2006. **83**(2): p. 461S-465S.
33. Clayton, P.E., et al., *Growth hormone, the insulin-like growth factor axis, insulin and cancer risk.* Nat Rev Endocrinol, 2011. **7**(1): p. 11-24.
34. J., N., *Molecular background of common dyslipidemias.*, in *Helsinki: National Public Health Institute*. 2008.
35. Trujillo, M.E. and P.E. Scherer, *Adipose Tissue-Derived Factors: Impact on Health and Disease.* Endocrine Reviews, 2006. **27**(7): p. 762-778.
36. Muc-Wierzgoń, M., et al., *Specific metabolic biomarkers as risk and prognostic factors in colorectal cancer.* World J Gastroenterol, 2014. **20**(29): p. 9759-74.
37. Nicholson, J.K., J.C. Lindon, and E. Holmes, *'Metabonomics': understanding the metabolic responses of living systems to pathophysiological stimuli via multivariate statistical analysis of biological NMR spectroscopic data.* Xenobiotica, 1999. **29**(11): p. 1181-9.
38. Kawakami, H., A. Zaanan, and F.A. Sinicrope, *Implications of mismatch repair-deficient status on management of early stage colorectal cancer.* Journal of Gastrointestinal Oncology, 2015. **6**(6): p. 676-684.
39. Chen, W., et al., *Study on metabonomic characteristics of human lung cancer using high resolution magic-angle spinning 1H NMR spectroscopy and multivariate data analysis.* Magnetic Resonance in Medicine, 2011. **66**(6): p. 1531-1540.
40. Phipps, A.I., et al., *KRAS-mutation status in relation to colorectal cancer survival: the joint impact of correlated tumour markers.* Br J Cancer, 2013. **108**(8): p. 1757-64.
41. Rosty, C., et al., *Colorectal carcinomas with KRAS mutation are associated with distinctive morphological and molecular features.* Mod Pathol, 2013. **26**(6): p. 825-34.
42. De Roock, W., et al., *Effects of KRAS, BRAF, NRAS, and PIK3CA mutations on the efficacy of cetuximab plus chemotherapy in chemotherapy-refractory metastatic colorectal cancer: a retrospective consortium analysis.* Lancet Oncol, 2010. **11**(8): p. 753-62.
43. De Roock, W., et al., *KRAS, BRAF, PIK3CA, and PTEN mutations: implications for targeted therapies in metastatic colorectal cancer.* Lancet Oncol, 2011. **12**(6): p. 594-603.

44. Grothey, A., *EGFR Antibodies in Colorectal Cancer: Where Do They Belong?* Journal of Clinical Oncology, 2010. **28**(31): p. 4668-4670.
45. Boland, C.R. and A. Goel, *Microsatellite instability in colorectal cancer.* Gastroenterology, 2010. **138**(6): p. 2073-2087.e3.
46. Funkhouser, W.K., Jr., et al., *Relevance, pathogenesis, and testing algorithm for mismatch repair-defective colorectal carcinomas: a report of the association for molecular pathology.* J Mol Diagn, 2012. **14**(2): p. 91-103.
47. Sepulveda, A.R., et al., *Molecular Biomarkers for the Evaluation of Colorectal Cancer: Guideline Summary From the American Society for Clinical Pathology, College of American Pathologists, Association for Molecular Pathology, and American Society of Clinical Oncology.* Journal of Oncology Practice, 2017. **13**(5): p. 333-337.
48. Bartel, D.P., *MicroRNAs: genomics, biogenesis, mechanism, and function.* Cell, 2004. **116**(2): p. 281-97.
49. Huang, Q., et al., *The microRNAs miR-373 and miR-520c promote tumour invasion and metastasis.* Nat Cell Biol, 2008. **10**(2): p. 202-10.
50. Lee, D.Y., et al., *MicroRNA-378 promotes cell survival, tumor growth, and angiogenesis by targeting SuFu and Fus-1 expression.* Proceedings of the National Academy of Sciences, 2007. **104**(51): p. 20350-20355.
51. Ma, L., J. Teruya-Feldstein, and R.A. Weinberg, *Tumour invasion and metastasis initiated by microRNA-10b in breast cancer.* Nature, 2007. **449**(7163): p. 682-8.
52. Yu, S.L., et al., *MicroRNA signature predicts survival and relapse in lung cancer.* Cancer Cell, 2008. **13**(1): p. 48-57.
53. Slaby, O., et al., *MicroRNAs in colorectal cancer: translation of molecular biology into clinical application.* Mol Cancer, 2009. **8**: p. 102.
54. Slaby, O., et al., *Altered expression of miR-21, miR-31, miR-143 and miR-145 is related to clinicopathologic features of colorectal cancer.* Oncology, 2007. **72**(5-6): p. 397-402.
55. Schetter, A.J., et al., *MicroRNA Expression Profiles Associated With Prognosis and Therapeutic Outcome in Colon Adenocarcinoma.* JAMA, 2008. **299**(4): p. 425-436.
56. Benjamin, R.S., et al., *We Should Desist Using RECIST, at Least in GIST.* Journal of Clinical Oncology, 2007. **25**(13): p. 1760-1764.
57. O'Connor, J.P., et al., *Quantitative imaging biomarkers in the clinical development of targeted therapeutics: current and future perspectives.* Lancet Oncol, 2008. **9**(8): p. 766-76.
58. Patel, U.B., et al., *MRI after treatment of locally advanced rectal cancer: how to report tumor response--the MERCURY experience.* AJR Am J Roentgenol, 2012. **199**(4): p. W486-95.
59. Goh, V. and R. Glynne-Jones, *Perfusion CT imaging of colorectal cancer.* Br J Radiol, 2014. **87**(1034): p. 20130811.
60. George, M.L., et al., *Non-invasive methods of assessing angiogenesis and their value in predicting response to treatment in colorectal cancer.* Br J Surg, 2001. **88**(12): p. 1628-36.
61. Goh, V., et al., *Can perfusion CT assessment of primary colorectal adenocarcinoma blood flow at staging predict for subsequent metastatic disease? A pilot study.* Eur Radiol, 2009. **19**(1): p. 79-89.
62. Hayano, K., et al., *Quantitative measurement of blood flow using perfusion CT for assessing clinicopathologic features and prognosis in patients with rectal cancer.* Dis Colon Rectum, 2009. **52**(9): p. 1624-9.
63. Mandard, A.M., et al., *Pathologic assessment of tumor regression after preoperative chemoradiotherapy of esophageal carcinoma. Clinicopathologic correlations.* Cancer, 1994. **73**(11): p. 2680-6.
64. McClelland, D. and G.I. Murray, *A Comprehensive Study of Extramural Venous Invasion in Colorectal Cancer.* PLoS One, 2015. **10**(12): p. e0144987.
65. Benson, A.B., 3rd, et al., *American Society of Clinical Oncology recommendations on adjuvant chemotherapy for stage II colon cancer.* J Clin Oncol, 2004. **22**(16): p. 3408-19.

66. Sun, Y.S., et al., *Locally advanced rectal carcinoma treated with preoperative chemotherapy and radiation therapy: preliminary analysis of diffusion-weighted MR imaging for early detection of tumor histopathologic downstaging.* Radiology, 2010. **254**(1): p. 170-8.
67. Hein, P.A., et al., *Diffusion-weighted magnetic resonance imaging for monitoring diffusion changes in rectal carcinoma during combined, preoperative chemoradiation: preliminary results of a prospective study.* Eur J Radiol, 2003. **45**(3): p. 214-22.
68. Baliyan, V., et al., *Diffusion weighted imaging: Technique and applications.* World J Radiol, 2016. **8**(9): p. 785-798.
69. Ichikawa, T., et al., *High-B-value diffusion-weighted MRI in colorectal cancer.* AJR Am J Roentgenol, 2006. **187**(1): p. 181-4.
70. Joye, I., et al., *The role of diffusion-weighted MRI and (18)F-FDG PET/CT in the prediction of pathologic complete response after radiochemotherapy for rectal cancer: a systematic review.* Radiother Oncol, 2014. **113**(2): p. 158-65.
71. Meng, X., et al., *Prediction of response to preoperative chemoradiotherapy in patients with locally advanced rectal cancer.* Biosci Trends, 2014. **8**(1): p. 11-23.
72. Hardie, A.D., et al., *Diagnosis of liver metastases: value of diffusion-weighted MRI compared with gadolinium-enhanced MRI.* Eur Radiol, 2010. **20**(6): p. 1431-41.
73. Anzidei, M., et al., *Liver metastases from colorectal cancer treated with conventional and antiangiogenetic chemotherapy: evaluation with liver computed tomography perfusion and magnetic resonance diffusion-weighted imaging.* J Comput Assist Tomogr, 2011. **35**(6): p. 690-6.
74. Heijmen, L., et al., *Diffusion-weighted MR imaging in liver metastases of colorectal cancer: reproducibility and biological validation.* Eur Radiol, 2013. **23**(3): p. 748-56.
75. Koh, D.M., et al., *Detection of colorectal hepatic metastases using MnDPDP MR imaging and diffusion-weighted imaging (DWI) alone and in combination.* Eur Radiol, 2008. **18**(5): p. 903-10.
76. Taouli, B., et al., *Chronic hepatitis: role of diffusion-weighted imaging and diffusion tensor imaging for the diagnosis of liver fibrosis and inflammation.* J Magn Reson Imaging, 2008. **28**(1): p. 89-95.
77. Sitter, B., et al., *Quantification of metabolites in breast cancer patients with different clinical prognosis using HR MAS MR spectroscopy.* NMR Biomed, 2010. **23**(4): p. 424-31.
78. Kobayashi, T., et al., *A novel serum metabolomics-based diagnostic approach to pancreatic cancer.* Cancer Epidemiol Biomarkers Prev, 2013. **22**(4): p. 571-9.
79. Zhang, T., et al., *Identification of potential biomarkers for ovarian cancer by urinary metabolomic profiling.* J Proteome Res, 2013. **12**(1): p. 505-12.
80. Warburg, O., *On the origin of cancer cells.* Science, 1956. **123**(3191): p. 309-14.
81. Reivich, M. and A. Alavi, *Positron emission tomographic studies of local cerebral glucose metabolism in humans in physiological and pathophysiological conditions.* Adv Metab Disord, 1983. **10**: p. 135-76.
82. Cornelis, F., et al., *18F-FDG PET/CT Is an Immediate Imaging Biomarker of Treatment Success After Liver Metastasis Ablation.* J Nucl Med, 2016. **57**(7): p. 1052-7.
83. Wiesmüller, M., et al., *Comparison of lesion detection and quantitation of tracer uptake between PET from a simultaneously acquiring whole-body PET/MR hybrid scanner and PET from PET/CT.* Eur J Nucl Med Mol Imaging, 2013. **40**(1): p. 12-21.
84. Mirnezami, R., et al., *Rapid diagnosis and staging of colorectal cancer via high-resolution magic angle spinning nuclear magnetic resonance (HR-MAS NMR) spectroscopy of intact tissue biopsies.* Ann Surg, 2014. **259**(6): p. 1138-49.
85. Jiménez, B., et al., *1H HR-MAS NMR spectroscopy of tumor-induced local metabolic "field-effects" enables colorectal cancer staging and prognostication.* J Proteome Res, 2013. **12**(2): p. 959-68.

86. Ng, F., et al., *Assessment of primary colorectal cancer heterogeneity by using whole-tumor texture analysis: contrast-enhanced CT texture as a biomarker of 5-year survival.* Radiology, 2013. **266**(1): p. 177-84.
87. Ryu, J.H., et al., *Randomized clinical trial of immersive virtual reality tour of the operating theatre in children before anaesthesia.* Br J Surg, 2017. **104**(12): p. 1628-1633.
88. Devoto, L., S. Muscroft, and M. Chand, *Highly Accurate, Patient-Specific, 3-Dimensional Mixed-Reality Model Creation for Surgical Training and Decision-making.* JAMA Surg, 2019. **154**(10): p. 968-969.
89. Milgram, P.K., Fumio, *A TAXONOMY OF MIXED REALITY VISUAL DISPLAYS* IEICE Trans. Information Systems, 1994. **E77-D, no. 12**: p. 1321-1329.
90. Stephen Thompson, J.T., Yi Song, Stian Johnsen, Danail Stoyanov, Sébastien Ourselin, Kurinchi Gurusamy, Crispin Schneider, Brian Davidson, David Hawkes, and Matthew J. Clarkson *Accuracy validation of an image guided laparoscopy system for liver resection.* Proceedings of SPIE - The International Society for Optical Engineering. **9415**.
91. Franchini Melani, A.G., M. Diana, and J. Marescaux, *The quest for precision in transanal total mesorectal excision.* Tech Coloproctol, 2016. **20**(1): p. 11-8.
92. Mascagni, P., et al., *New intraoperative imaging technologies: Innovating the surgeon's eye toward surgical precision.* J Surg Oncol, 2018. **118**(2): p. 265-282.
93. Guerriero, L., et al., *Virtual Reality Exploration and Planning for Precision Colorectal Surgery.* Dis Colon Rectum, 2018. **61**(6): p. 719-723.
94. Bernhardt, S., et al., *The status of augmented reality in laparoscopic surgery as of 2016.* Med Image Anal, 2017. **37**: p. 66-90.
95. Sielhorst, T.F., Marco & Traub, Joerg & Kutter, Oliver & Navab, Nassir, *CAMPAR: A software framework guaranteeing quality for medical augmented reality (2006).* Int. J. Comput. Assist. Radiol. Surg, 2006: p. 29-30.
96. Zare-Bandamiri, M., et al., *Risk Factors Predicting Colorectal Cancer Recurrence Following Initial Treatment: A 5-year Cohort Study.* Asian Pac J Cancer Prev, 2017. **18**(9): p. 2465-2470.
97. Laubert, T., et al., *Metachronous metastasis- and survival-analysis show prognostic importance of lymphadenectomy for colon carcinomas.* BMC Gastroenterol, 2012. **12**: p. 24.
98. Devoto, L., et al., *Using texture analysis in the development of a potential radiomic signature for early identification of hepatic metastasis in colorectal cancer.* Eur J Radiol Open, 2022. **9**: p. 100415.
99. Slakey, D.P., et al., *Using simulation to improve root cause analysis of adverse surgical outcomes.* Int J Qual Health Care, 2014. **26**(2): p. 144-50.
100. Chung, K.C. and S.V. Kotsis, *Complications in surgery: root cause analysis and preventive measures.* Plast Reconstr Surg, 2012. **129**(6): p. 1421-1427.
101. Rose, A.S., et al., *Pre-operative simulation of pediatric mastoid surgery with 3D-printed temporal bone models.* Int J Pediatr Otorhinolaryngol, 2015. **79**(5): p. 740-4.
102. Feeney, G., et al., *Neoadjuvant radiotherapy for rectal cancer management.* World J Gastroenterol, 2019. **25**(33): p. 4850-4869.
103. Boland, P.M. and M. Fakih, *The emerging role of neoadjuvant chemotherapy for rectal cancer.* J Gastrointest Oncol, 2014. **5**(5): p. 362-73.
104. Nagtegaal, I.D. and R. Glynne-Jones, *How to measure tumour response in rectal cancer? An explanation of discrepancies and suggestions for improvement.* Cancer Treat Rev, 2020. **84**: p. 101964.
105. Nardone, L., et al., *A feasibility study of neo-adjuvant low-dose fractionated radiotherapy with two different concurrent anthracycline-docetaxel schedules in stage IIA/B-IIIA breast cancer.* Tumori, 2012. **98**(1): p. 79-85.
106. Dworak, O., L. Keilholz, and A. Hoffmann, *Pathological features of rectal cancer after preoperative radiochemotherapy.* Int J Colorectal Dis, 1997. **12**(1): p. 19-23.

107. Lee, Y.C., C.C. Hsieh, and J.P. Chuang, *Prognostic significance of partial tumor regression after preoperative chemoradiotherapy for rectal cancer: a meta-analysis.* Dis Colon Rectum, 2013. **56**(9): p. 1093-101.
108. Patel, U.B., et al., *MRI assessment and outcomes in patients receiving neoadjuvant chemotherapy only for primary rectal cancer: long-term results from the GEMCAD 0801 trial.* Ann Oncol, 2017. **28**(2): p. 344-353.
109. Han, Y.B., et al., *Clinical impact of tumor volume reduction in rectal cancer following preoperative chemoradiation.* Diagn Interv Imaging, 2016. **97**(9): p. 843-50.
110. Shiraishi, T., et al., *Predicting prognosis according to preoperative chemotherapy response in patients with locally advanced lower rectal cancer.* BMC Cancer, 2019. **19**(1): p. 1222.
111. De'Ath, H.D., et al., *Mentored Trainees have Similar Short-Term Outcomes to a Consultant Trainer Following Laparoscopic Colorectal Resection.* World J Surg, 2017. **41**(7): p. 1896-1902.
112. Datta, N., et al., *Wearable Technology for Global Surgical Teleproctoring.* J Surg Educ, 2015. **72**(6): p. 1290-5.
113. AlMazeedi, S.M., et al., *Employing augmented reality telesurgery for COVID-19 positive surgical patients.* Br J Surg, 2020. **107**(10): p. e386-e387.
114. Luck, J., N. Gosling, and S. Saour, *Undergraduate surgical education during COVID-19: could augmented reality provide a solution?* Br J Surg, 2021. **108**(3): p. e129-e130.
115. Okamura, A.M., *Haptic feedback in robot-assisted minimally invasive surgery.* Curr Opin Urol, 2009. **19**(1): p. 102-7.
116. Morland, D., et al., *Radiomics in Oncological PET Imaging: A Systematic Review-Part 1, Supradiaphragmatic Cancers.* Diagnostics (Basel), 2022. **12**(6).
117. Castellano, G., et al., *Texture analysis of medical images.* Clin Radiol, 2004. **59**(12): p. 1061-9.
118. Boehm, H.F., et al., *Automated classification of normal and pathologic pulmonary tissue by topological texture features extracted from multi-detector CT in 3D.* Eur Radiol, 2008. **18**(12): p. 2745-55.
119. Chen, S., et al., *Texture analysis of baseline multiphasic hepatic computed tomography images for the prognosis of single hepatocellular carcinoma after hepatectomy: A retrospective pilot study.* Eur J Radiol, 2017. **90**: p. 198-204.
120. Chae, H.D., et al., *Computerized texture analysis of persistent part-solid ground-glass nodules: differentiation of preinvasive lesions from invasive pulmonary adenocarcinomas.* Radiology, 2014. **273**(1): p. 285-93.
121. Dohan, A., et al., *Early evaluation using a radiomic signature of unresectable hepatic metastases to predict outcome in patients with colorectal cancer treated with FOLFIRI and bevacizumab.* Gut, 2020. **69**(3): p. 531-539.
122. Chee, C.G., et al., *CT texture analysis in patients with locally advanced rectal cancer treated with neoadjuvant chemoradiotherapy: A potential imaging biomarker for treatment response and prognosis.* PLoS One, 2017. **12**(8): p. e0182883.
123. Jalil, O., et al., *Magnetic resonance based texture parameters as potential imaging biomarkers for predicting long-term survival in locally advanced rectal cancer treated by chemoradiotherapy.* Colorectal Dis, 2017. **19**(4): p. 349-362.
124. Rao, S.X., et al., *CT texture analysis in colorectal liver metastases: A better way than size and volume measurements to assess response to chemotherapy?* United European Gastroenterol J, 2016. **4**(2): p. 257-63.
125. Guren, M.G., et al., *Nationwide improvement of rectal cancer treatment outcomes in Norway, 1993-2010.* Acta Oncol, 2015. **54**(10): p. 1714-22.
126. van der Geest, L.G., et al., *Nationwide trends in incidence, treatment and survival of colorectal cancer patients with synchronous metastases.* Clin Exp Metastasis, 2015. **32**(5): p. 457-65.
127. Robinson, P.J., *The early detection of liver metastases.* Cancer Imaging, 2002. **2**(2): p. 1-3.

128. Miles, K.A., B. Ganeshan, and M.P. Hayball, *CT texture analysis using the filtration-histogram method: what do the measurements mean?* Cancer Imaging, 2013. **13**(3): p. 400-6.
129. Andersen, M.B., et al., *CT texture analysis can help differentiate between malignant and benign lymph nodes in the mediastinum in patients suspected for lung cancer.* Acta Radiol, 2016. **57**(6): p. 669-76.
130. Haider, M.A., et al., *CT texture analysis: a potential tool for prediction of survival in patients with metastatic clear cell carcinoma treated with sunitinib.* Cancer Imaging, 2017. **17**(1): p. 4.
131. Smith, A.D., et al., *Predicting Overall Survival in Patients With Metastatic Melanoma on Antiangiogenic Therapy and RECIST Stable Disease on Initial Posttherapy Images Using CT Texture Analysis.* AJR Am J Roentgenol, 2015. **205**(3): p. W283-93.
132. Hayano, K., et al., *Texture Analysis of Non-Contrast-Enhanced Computed Tomography for Assessing Angiogenesis and Survival of Soft Tissue Sarcoma.* J Comput Assist Tomogr, 2015. **39**(4): p. 607-12.
133. Ganeshan, B., et al., *Hepatic enhancement in colorectal cancer: texture analysis correlates with hepatic hemodynamics and patient survival.* Acad Radiol, 2007. **14**(12): p. 1520-30.
134. Chand, M., et al., *Extramural venous invasion is a potential imaging predictive biomarker of neoadjuvant treatment in rectal cancer.* Br J Cancer, 2014. **110**(1): p. 19-25.
135. Oshowo, A., et al., *Comparison of resection and radiofrequency ablation for treatment of solitary colorectal liver metastases.* Br J Surg, 2003. **90**(10): p. 1240-3.
136. van Gijn, W., et al., *Nomograms to predict survival and the risk for developing local or distant recurrence in patients with rectal cancer treated with optional short-term radiotherapy.* Ann Oncol, 2015. **26**(5): p. 928-935.
137. Nakajo, M., et al., *A pilot study for texture analysis of (18)F-FDG and (18)F-FLT-PET/CT to predict tumor recurrence of patients with colorectal cancer who received surgery.* Eur J Nucl Med Mol Imaging, 2017. **44**(13): p. 2158-2168.
138. Association, N.E.M. *National Electrical Manufacturers Association About DICOM: Overview.* . 2020 [cited 2022 29/08/2022]; Available from: https://www.dicomstandard.org/current
139. Caffery, L.J., et al., *The Role of DICOM in Artificial Intelligence for Skin Disease.* Front Med (Lausanne), 2020. **7**: p. 619787.
140. Schreiber, J.J., et al., *Hounsfield units for assessing bone mineral density and strength: a tool for osteoporosis management.* J Bone Joint Surg Am, 2011. **93**(11): p. 1057-63.
141. Raffan, H., et al., *Canine neuroanatomy: Development of a 3D reconstruction and interactive application for undergraduate veterinary education.* PLoS One, 2017. **12**(2): p. e0168911.
142. Teeling, K.P., D. Werling, and D. Berner, *Preliminary Volumetric Calculation of the Mucosal Surface in the Nares of Lambs Using a Segmentation of Computed Tomographic Images.* Front Vet Sci, 2020. **7**: p. 620647.
143. Kelly, P.J., et al., *Computer-assisted stereotaxic laser resection of intra-axial brain neoplasms.* J Neurosurg, 1986. **64**(3): p. 427-39.
144. Winne, C., et al., *Overlay visualization in endoscopic ENT surgery.* Int J Comput Assist Radiol Surg, 2011. **6**(3): p. 401-6.
145. Wengert, C., et al., *Markerless endoscopic registration and referencing.* Med Image Comput Comput Assist Interv, 2006. **9**(Pt 1): p. 816-23.
146. Zinser, M.J., et al., *A paradigm shift in orthognathic surgery? A comparison of navigation, computer-aided designed/computer-aided manufactured splints, and "classic" intermaxillary splints to surgical transfer of virtual orthognathic planning.* J Oral Maxillofac Surg, 2013. **71**(12): p. 2151.e1-21.
147. Marescaux, J., et al., *Augmented-reality-assisted laparoscopic adrenalectomy.* Jama, 2004. **292**(18): p. 2214-5.
148. Sánchez-Margallo, F.M., et al., *Anatomical changes due to pneumoperitoneum analyzed by MRI: an experimental study in pigs.* Surg Radiol Anat, 2011. **33**(5): p. 389-96.

149. Sugimoto, M., et al., *Image overlay navigation by markerless surface registration in gastrointestinal, hepatobiliary and pancreatic surgery.* J Hepatobiliary Pancreat Sci, 2010. **17**(5): p. 629-36.
150. Volonté, F., et al., *Augmented reality and image overlay navigation with OsiriX in laparoscopic and robotic surgery: not only a matter of fashion.* J Hepatobiliary Pancreat Sci, 2011. **18**(4): p. 506-9.
151. Weiss, C.R., et al., *Augmented reality visualization using Image-Overlay for MR-guided interventions: system description, feasibility, and initial evaluation in a spine phantom.* AJR Am J Roentgenol, 2011. **196**(3): p. W305-7.
152. Birkfellner, W., et al., *Computer-enhanced stereoscopic vision in a head-mounted operating binocular.* Phys Med Biol, 2003. **48**(3): p. N49-57.
153. Muensterer, O.J., et al., *Google Glass in pediatric surgery: an exploratory study.* Int J Surg, 2014. **12**(4): p. 281-9.
154. Tanagho, Y.S., et al., *2D versus 3D visualization: impact on laparoscopic proficiency using the fundamentals of laparoscopic surgery skill set.* J Laparoendosc Adv Surg Tech A, 2012. **22**(9): p. 865-70.
155. Alaraimi, B., et al., *A randomized prospective study comparing acquisition of laparoscopic skills in three-dimensional (3D) vs. two-dimensional (2D) laparoscopy.* World J Surg, 2014. **38**(11): p. 2746-52.
156. Ali, M.R., et al., *3-D telestration: a teaching tool for robotic surgery.* J Laparoendosc Adv Surg Tech A, 2008. **18**(1): p. 107-12.
157. nvidia.com. *Developer.download.nvidia.com. (2007). GPU Gems - Chapter 39. Volume Rendering Techniques*. 2018 [cited 2018 Accessed 4 Apr. 2018]; Available from: http://developer.download.nvidia.com/books/HTML/gpugems/gpugems_ch39.html
158. Kruger, J.a.W., R. *Acceleration Techniques for GPU-based Volume Rendering*. 2003 4 Apr. 2018]; Available from: https://dl.acm.org/citation.cfm?id=1081482
159. Kim, S. and P. Kazanzides, *Fiducial-based registration with a touchable region model.* Int J Comput Assist Radiol Surg, 2017. **12**(2): p. 277-289.
160. Kong, S.H., et al., *Robust augmented reality registration method for localization of solid organs' tumors using CT-derived virtual biomechanical model and fluorescent fiducials.* Surg Endosc, 2017. **31**(7): p. 2863-2871.
161. Decker, R.S., et al., *Biocompatible Near-Infrared Three-Dimensional Tracking System.* IEEE Trans Biomed Eng, 2017. **64**(3): p. 549-556.
162. Kobayashi, S., et al., *Survival Benefit of and Indications for Adjuvant Chemotherapy for Resected Colorectal Liver Metastases-a Japanese Nationwide Survey.* J Gastrointest Surg, 2020. **24**(6): p. 1244-1260.
163. Zhang, Y., et al., *Neoadjuvant chemotherapy for patients with resectable colorectal cancer liver metastases: A systematic review and meta-analysis.* World J Clin Cases, 2021. **9**(22): p. 6357-6379.
164. Claassen, Y., et al., *Survival differences with immediate versus delayed chemotherapy for asymptomatic incurable metastatic colorectal cancer.* Cochrane Database Syst Rev, 2016. **2016**(10).
165. Ackland, S.P., et al., *A meta-analysis of two randomised trials of early chemotherapy in asymptomatic metastatic colorectal cancer.* Br J Cancer, 2005. **93**(11): p. 1236-43.
166. Meling, T.R. and T.R. Meling, *The impact of surgical simulation on patient outcomes: a systematic review and meta-analysis.* Neurosurg Rev, 2021. **44**(2): p. 843-854.
167. Moldovanu, R., et al., *Preoperative warm-up using a virtual reality simulator.* Jsls, 2011. **15**(4): p. 533-8.
168. Laudicella, M., et al., *Cost of care for cancer patients in England: evidence from population-based patient-level data.* Br J Cancer, 2016. **114**(11): p. 1286-92.

169. Nogueira-Reis, F., et al., *Three-dimensional maxillary virtual patient creation by convolutional neural network-based segmentation on cone-beam computed tomography images.* Clin Oral Investig, 2022.
170. Whittaker, T.M., et al., *Delay to elective colorectal cancer surgery and implications for survival: a systematic review and meta-analysis.* Colorectal Dis, 2021. **23**(7): p. 1699-1711.
171. Chen, S., et al., *Can virtual reality improve traditional anatomy education programmes? A mixed-methods study on the use of a 3D skull model.* BMC Med Educ, 2020. **20**(1): p. 395.

Appendix 1 CT Texture Analysis of Patients Who Did and Did Not Develop Hepatic Metastasis

Characteristic Data	Metastasis	No Metastasis	p-value
No filtration			
TX_sigma			
mean	95.68	92.29	0.091
Standard Deviation	14.64	14.29	0.740
Entropy	4.055	4.06	0.880
MPP	95.68	92.29	0.091
Skewness	0.41	0.27	0.211
Kurtosis	0.99	0.76	0.169
Filter 2.0 (fine)			0.211
TX_sigma			
mean	1.31	0.74	0.235
Standard Deviation	33.57	29.29	0.091
Entropy	4.89	4.78	0.134
MPP	27.08	23.43	0.091
Skewness	0.62	0.29	0.118
Kurtosis	1.72	0.95	0.288
Filter 3.0 (med)			
TX_sigma			
mean	3.58	2.06	0.091
Standard Deviation	30.04	25.59	0.069

Entropy	4.71	4.58	0.059
MPP	24.63	21.57	**0.023**
Skewness	1.19	1.08	0.413
Kurtosis	3.27	3.19	1.000
Filter 4.0 (med)			
TX_sigma			
mean	6.86	4.04	0.051
Standard Deviation	30.37	24.17	**0.032**
Entropy	4.66	4.51	0.059
MPP	26.07	19.99	**0.044**
Skewness	1.27	1.39	0.880
Kurtosis	3.18	3.70	0.379
Filter 5.0 (med)			
TX_sigma			
mean	10.35	6.13	**0.044**
Standard Deviation	32.78	24.81	**0.016**
Entropy	4.71	4.52	0.069
MPP	29.47	21.66	**0.019**
Skewness	1.18	1.34	0.740
Kurtosis	2.63	3.56	0.134
Filter 6.0 (coarse)			
TX_sigma			

mean	13.85	7.98	**0.044**
Standard Deviation	35.31	25.71	**0.013**
Entropy	4.77	4.55	**0.032**
MPP	32.96	23.04	**0.007**
Skewness	1.09	1.20	0.880
Kurtosis	2.31	2.27	0.413

Appendix 2 **M**ixed **R**eality **SU**rgical **R**esection **G**uidance MR SURG; Evaluation questionnaire; Statements are evaluated on a 5-point Likert scale: 1 = fully disagree, 2 = disagree, 3 = neutral, 4 = agree, 5 = fully agree

The system was user friendly	Score 1-5
The system was easy to control	Score 1-5
Images were clearly visible	Score 1-5
The model anatomy was easy to understand	Score 1-5
I was able to visualise all the specific anatomical structures relevant to the operation	Score 1-5
The system added useful information at the time of operation	Score 1-5
The system helped guide the surgery	Score 1-5
The system was not a distraction when used at the time of surgery	Score 1-5
Overall, the system was useful for this surgery	Score 1-5
I would like to use a mixed reality model for other surgeries	Score 1-5

Appendix 3 Video of the patient specific model being viewed prior to surgery

hololens model trim.mp4

Appendix 4 Video of the creation and intraoperative use of the patient specific model

Model creation and use video.wmv

Appendix 5 Video of a partially co-registered patient model during surgery

AR-HOLO-UCHL-01.mp4